Origins, evolutions, and future directions of Landsat science products for advancing global inland water and coastal ocean observations

Benjamin Page[1] (0000-0002-9871-2406), Christopher J. Crawford[2] (0000-0002-7145-0709), Saeed Arab[3] (0000-0003-1602-8801), Gail Schmidt[3] (0000-0002-9684-8158), Christopher Barnes[3] (0000-0002-4608-4364), Danika Wellington[3] (0000-0002-2130-0075)

[1]Earth Space Technology Services (ESTS), Contractor to the USGS EROS Center, Sioux Falls, SD, 57198, USA
[2]U.S. Geological Survey (USGS) Earth Resources Observation and Science (EROS) Center, 47914 252nd Street, Sioux Falls, SD, 57198, USA
[3]KBR, Inc., Contractor to the USGS EROS Center, Sioux Falls, SD, 57198, USA

Correspondence to: Benjamin P. Page (bpage@contractor.usgs.gov)

Abstract. In April 2020, the U.S. Geological Survey (USGS) Earth Resources Observation and Science (EROS) Center introduced a Level 2 provisional Aquatic Reflectance (AR) product for the Landsat 8 Operational Land Imager (OLI), marking the initial phase in developing a standardized global product for Landsat-derived surface water measurements. The goal of USGS EROS aquatic product research and development is to prepare for an operational processing architecture for Landsat Collection 3 in the late 2020s that will enable use of quality-controlled data for emerging Landsat aquatic science applications. To achieve this, we released a subset of the Landsat 8/9 provisional AR products and examined its general performance through the Science Algorithms to Operations (SATO) framework alongside quantitative assessment using community made inland water data records (GLObal Reflectance community dataset for Imaging and optical sensing of Aquatic environments, GLORIA) and radiometric coastal validation platforms (NASA's Ocean Color component of the Aerosol Robotic Network, AERONET-OC). Variability within the validation datasets indicate that the performance of the Landsat 8/9 provisional AR retrieval is highly context-dependent; errors are minimal in optically simple waters (e.g., clear to moderately turbid coastal waters) but increase considerably in optically complex waters where factors such as elevated levels of turbidity, chlorophyll (Chl-a) concentrations, or colored dissolved organic matter (CDOM) dominate the water column. Additionally, this paper examines key algorithmic considerations for atmospheric correction, highlighting factors that influence accuracy, scalability, and computational efficiency necessary for collection processing in the operational Landsat Product Generation System (LPGS). This paper is intended to communicate with aquatic scientists, satellite oceanographers, and the broader Earth observation community on the origins, requirements, challenges, successes, and future objectives for operationalizing global AR data products for Landsat satellite missions.

1 Introduction

For over a half-century, the Landsat program, a series of joint agency Earth observing satellite missions between the National Aeronautics and Space Administration (NASA) and the U.S. Geological Survey (USGS), has provided high-quality global land and nearshore coastal observations from a suite of medium-resolution imaging satellites (Wulder et al., 2022; Crawford et al., 2023). Upon the adoption of a collection-based archive processing and management approach in 2016 (Dwyer et al. 2018; Crawford et al. 2023), Landsat data are systematically processed, archived, and distributed by the USGS Earth Resources Observation and Science (EROS) Center located in Sioux Falls, South Dakota, USA. Through collaboration with remote sensing subject matter experts and participation from the Landsat Science Team, USGS EROS has developed and operationalized research-quality Level 1 Top of Atmosphere (TOA) calibrated reflectance and Level 2 atmospherically corrected surface reflectance and surface temperature products that can be used to map, monitor, assess, and interpret how Earth's surface has changed as a result of human influence and natural environmental conditions. These open access data products from Landsat are made publicly available at no cost (Zhu et al. 2019) through the USGS EROS Earth Explorer (EE) data portal and Machine-to-Machine (M2M) Application Programming Interface (API). USGS also offers direct access to Landsat data through the Amazon Web Services (AWS) commercial cloud environment in a "Requester Pays" (user incurs cost for data requests and downloads) bucket configuration (Crawford et al. 2023). This allows researchers, scientists, U.S. federal and state agencies, and international organizations to utilize Landsat data products for their science applications, and to facilitate informed land, natural resources, and water management decisions and policies (Wulder et al. 2019).

Landsat Level 2 science product development follows a structured process that involves iterative collaboration between principal investigator(s) (e.g., a Landsat Science Team member or a U.S. federal agency scientist) and the USGS Landsat science project to operationalize mature science algorithms. The development phases of this process (discussed in Section 2) include research, provisional, and operational readiness levels for the generation of science data products. Products that are considered provisional are available to the public through the EROS Science Processing Architecture (ESPA; https://espa.cr.usgs.gov) on-demand interface but are actively under USGS internal evaluation and remote sensing community validation. These algorithms and the resulting product layers may undergo further modifications or improvements before being considered for operational release.

Although Landsat missions have primarily been designed for observing and monitoring land change, Landsat 8 (launched February 2013) and Landsat 9 (launched September 2021) have been used extensively for aquatic remote sensing applications (Tyler et al., 2022) due to the Operational Land Imager (OLI)'s substantial improvements in both radiometric data quality and spectral resolution compared to heritage Thematic Mapper (TM) and Enhanced Thematic Mapper Plus (ETM+) instruments (Roy et al., 2014; Pahlevan et al., 2014; Concha et al., 2016; Olmanson et al., 2016). Compensating for the intervening effects of atmospheric scattering and absorption between the sun, surface, and remote imaging sensor, which vary spatially and

65 temporally, is a necessary processing step to enable reliable monitoring, characterization, and interpretation of the Earth's surface (Vermote et al., 2008; Korkin and Lyapustin, 2023; Thompson et al., 2019; Thompson et al., 2022; Pahlevan et al., 2017). In contrast to brighter terrestrial land surfaces, retrieving atmospherically corrected spectral reflectance information from dark aquatic targets using spaceborne imaging sensors is a major challenge because the attenuated sunlight reflected from the water is usually only a fraction of the total signal received at the top of atmosphere (Wang, 2010).

70

In April 2020, USGS EROS introduced a Level 2 provisional Aquatic Reflectance (AR) product for Landsat 8 OLI observations, marking the initial phase in developing a standardized global product for Landsat-derived surface water measurements. The algorithm to generate AR products for Landsat 8 (and Landsat 9 since launch in September 2021) OLI imagery was adopted from version 8.10.3 of the Level 2 Generation (l2gen) module within the SeaWiFS Data Analysis System

75 (SeaDAS), originally developed by the NASA Ocean Biology Processing Group (OBPG). This software has been the standard processing method for several previous and ongoing NASA ocean color missions like the Coastal Zone Color Scanner (CZCS, 1978–1986), the Medium Resolution Imaging Spectrometer (MERIS, 2002–2012), the Geostationary Ocean Color Imager (GOCI, 2010–2021), the Moderate Resolution Imaging Spectroradiometer Aqua (MODIS Aqua, 2002–present), and the Visible Infrared Imaging Radiometer Suite (VIIRS, 2011–present) (Mobley et al., 2016). USGS Level 2 provisional AR

80 products have been available to process and download from the USGS ESPA on-demand interface. These products underwent a refresh in 2022 following the release of Landsat Collection 2 and contain Level 2 AR for the visible to near-infrared (VNIR) spectral bands (OLI bands 1–5) (Fig. 1), intermediate Rayleigh-corrected reflectance (ρrc) for the visible to shortwave infrared (VSWIR) spectral bands (OLI bands 1–7), and other supporting data layers. These provisional AR products are intended for immediate, experimental use by the remote sensing community involved in water quality monitoring, seafloor classification,

85 satellite derived bathymetry, and other surface water mapping applications so that community assessment of their suitability can be used to strengthen AR retrieval performance to operational readiness in support of applications requiring high quality measurements. Water quality surveying groups like the USGS Water Mission Area already rely on Landsat and Sentinel-2 observations to monitor U.S. national waters (Fickas et al., 2023; Stengel et al., 2023; Meyer et al., 2024), emphasizing the need for operationally generated satellite-derived data in enabling comprehensive and consistent water resource management

90 and assessments.

Satellite-derived AR measurements are a critical asset where *in situ* data are scarce or costly to collect. Feedback from science applications end users ensures that data outputs are both robust and actionable, fostering trust and reliability across scientific, policy, and operational domains. The goal of USGS EROS aquatic product research and development is to enable emerging

95 Landsat aquatic science applications and prepare for an operational processing architecture for Landsat Collection 3 in the late 2020s. The purpose of this paper is to communicate with aquatic scientists, satellite oceanographers, and the broader Earth observation community on the origins, requirements, challenges, successes, and future objectives for operationalizing global AR data products for Landsat satellite missions.
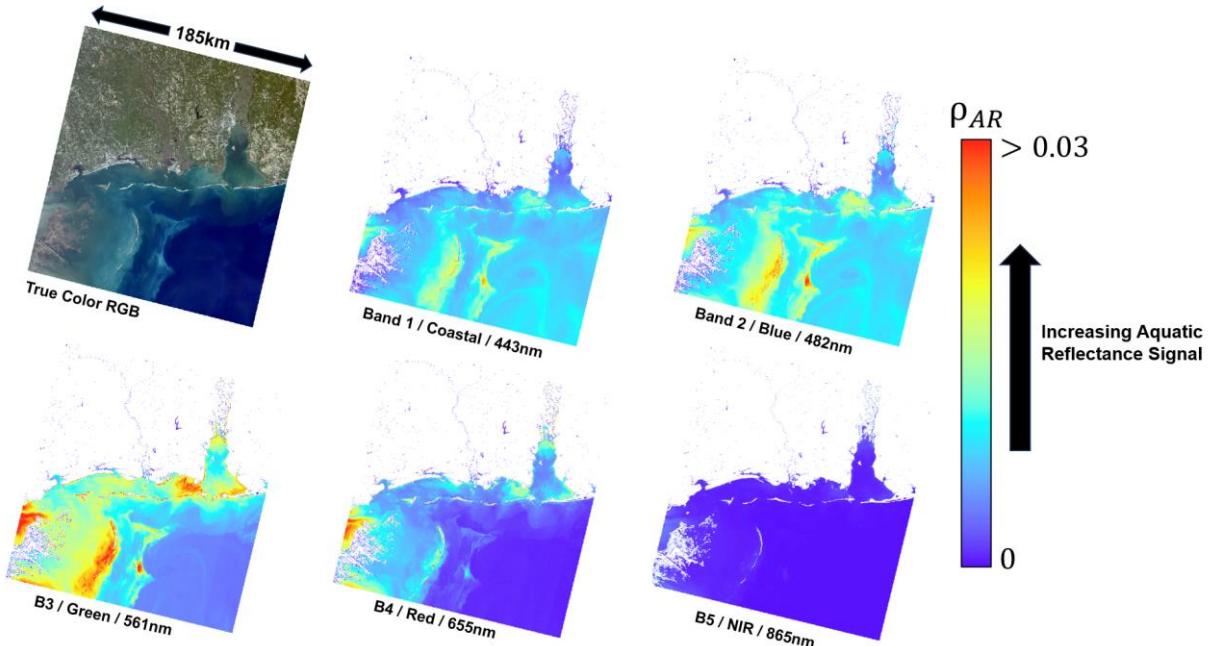
100

Figure 1. Example of the Landsat 8/9 Level 2 provisional Aquatic Reflectance product over coastal Alabama on November 15th, 2021. The Landsat 8/9 Level 2 provisional AR product package includes AR for the five OLI visible and near infrared (VNIR) bands centered at 443nm (coastal/aerosol), 482nm (blue), 561nm (green), 655nm (red), and 865nm (NIR) for identified water pixels at 30-meter spatial resolution. *Landsat image courtesy of the U.S. Geological Survey.*

2 Landsat provisional aquatic reflectance algorithm description and implementation

105

Remote sensing reflectance (R_{rs}) is defined as the ratio of the spectral distribution of reflected solar radiation upwelling from just beneath the water surface (L_w, W·m−2·sr-1) normalized by the downwelling solar irradiance (E_d, W·m−2) in the visible to near-infrared domain (λ=400–900 nm, unit: steradian-1) (Lee et al., 1997; Gordon and Wang, 1994; Mobley 1999):

$$R_{rs}(\lambda) = \frac{L_w(\lambda)}{E_d(\lambda)} \ (sr^{-1}), \qquad (1)$$

110   R_{rs} is the conventional measurement used in proximal, airborne, and satellite-based remote sensing to quantify the optically active, biogeochemical constituents (i.e., chlorophyll, total suspended solids, dissolved organic matter) (O'Reilly et al., 1998; Lee et al., 2001; Mishra and Mishra, 2012; Dogliotti et al., 2015) and is an essential component for the water quality analysis of lakes (Lehmann et al., 2018; Giardino et al., 2019), long term ocean color monitoring programs (Werdell et al., 2007), benthic mapping practices (Louchard et al., 2003; Dierssen et al., 2010), and optical water type classification for global water

115 bodies (Spyrakos et al., 2018; Bi and Hieronymi, 2024).

SeaDAS, developed and maintained by NASA's OBPG, is the satellite image preprocessing software for generating aquatic R_{rs} image products for several ocean color missions primarily associated with global monitoring programs for over 25 years (Mobley et al., 2016). Because of this, the open source code for l2gen supports several multispectral (and hyperspectral) Earth

120 Observation missions, including the OLI instruments onboard Landsat 8 and Landsat 9. The adaptation of l2gen processing for use with Landsat OLI data is described by Franz et al. (2015), with additional regional analyses of the impact of band selection for aerosol estimation provided by Vanhellemont et al. (2014) and Pahlevan et al. (2017).

The l2gen processing code within SeaDAS computes the R_{rs} for each band at each identified water pixel from the Level 1 at-

125 sensor radiance L_t, which is assumed to be partitioned linearly into distinct physical contributions as shown below:

$$L_t(\lambda) = [L_r(\lambda) + L_a(\lambda) + t_{dv}(\lambda)L_{wc}(\lambda) + t_{dv}(\lambda)L_w(\lambda)]\, t_{gv}(\lambda)t_{gs}(\lambda)f_p(\lambda), \qquad (2)$$

$L_r(\lambda)$ = the radiance contribution due to Rayleigh scattering by air molecules

$L_a(\lambda)$ = the contribution due to scattering by aerosols, including multiple scattering interactions with air molecules

$L_{wc}(\lambda)$ = the contribution from water surface whitecaps and foam

130 $L_w(\lambda)$ = the water-leaving component

$t_{dv}(\lambda)$ = the transmittance of diffuse radiation through the atmosphere in the viewing path from water surface to sensor

$t_{gv}(\lambda)$ = the transmittance loss due to absorbing gases for all upwelling radiation traveling along the sensor view path

$t_{gs}(\lambda)$ = the transmittance to the downwelling solar radiation due to the presence of absorbing gases along the path from Sun to the water surface

135 $f_p(\lambda)$ = an adjustment for effects of polarization

The l2gen atmospheric correction algorithm retrieves the water-leaving radiance L_w component of interest by estimating and subtracting the terms on the right-hand side of equation (2) from L_t. Of these components, the estimation of the aerosol scattering contribution L_a is generally the most challenging and impactful for the retrieval of L_w (outside of glint-contaminated areas, that is). While the l2gen software accepts a wide variety of processing options for aerosol radiance estimation, the

140 parameterization most commonly used in the operational processing of supported mission data makes use of an iterative bio-optical model to satisfy a fundamental assumption of the algorithmic approach: that near-infrared water-leaving radiance is either negligible or can be accurately estimated (Bailey et al. 2010). With this assumption, the aerosol radiance in each band can be estimated via the two-band aerosol selection approach of Gordon and Wang (1994). USGS provisional AR processing

uses OLI band 5 (865 nm) and band 6 (1609 nm) as the choice of bands, following the recommendation of Pahlevan et al.
(2017). The value of $R_{rs}(\lambda)$ is then computed as:

$$R_{rs}(\lambda) = \frac{L_w(\lambda)}{F_0(\lambda)\, f_s\, cos(\theta_s)\, t\,(\theta)}, \qquad (3)$$

where:

F_0 = extraterrestrial solar irradiance (Thuillier et al., 2003)

F_s = adjustment of F_0 for variation in Earth-Sun distance

t = diffuse transmittance

The spectral R_{rs} bands (in steradian) are normalized (multiplied by π) to produce dimensionless aquatic reflectance (Franz et al., 2007; Franz et al., 2015; Mobley et al., 2016):

$$Aquatic\ Reflectance\ AR(\lambda) = R_{rs}(\lambda) * \pi, \qquad (4)$$

Additional details, including the full set of processing parameters used in the generation of the provisional AR products, can be found in USGS documentation (USGS, 2024).

Due to its interoperability, traceability, and availability, the l2gen algorithm in SeaDAS (SeaDAS l2gen 8.10.3) was adopted by the USGS into the EROS's Science Algorithms to Operations (SATO) process in 2018, as a baseline for developing an atmospheric correction pathway for Landsat AR. The SATO Product Maturity Matrix for USGS Landsat science products is the formal description of the development process used by USGS EROS to mature algorithms for collection processing in the operational Landsat Product Generation System (LPGS). The purpose of SATO is to enable a smooth transition of researched, developed, and matured science algorithms and prototype executables into a formally developed and maintained LPGS operational environment. The product maturity matrix for provisional Landsat science products is adopted from the National Oceanic and Atmospheric Administration (NOAA) Climate Data Record (CDR) maturity model (Bates & Privette, 2012) and is used as the template to transition select candidate science algorithms through the SATO process (Table 1).

Maturity Level		Software Readiness	Metadata	Documentation	Product Validation	Public Access	Utility
Research	1	Conceptual Development	Little or none	Draft Algorithm Theoretical Basis Document (ATBD); paper on algorithm submitted	Little or None	Restricted to a select few	Little or none
	2	Significant code changes expected	Research grade	ATBD Version 1+; paper on algorithm reviewed	Minimal	Limited data availability to develop familiarity	Limited or ongoing

		Software	Dataset	Documentation	Uncertainty	Data Access	Applications
Provisional	3	Moderate code changes expected	Research grade, meets international standards	Public ATBD; peer-reviewed publication on algorithm	Uncertainty estimated for select locations / time	Data and source code archived and available; caveats required for use	Assessments have demonstrated positive values
	4	Some code changes expected	Exists at collection level. Stable. Allows provenance tracking and reproducibility of dataset. Meets international standards for dataset	Public ATBD; Draft Algorithm Description Document (ADD) and Product Guide (PG); peer-reviewed publication on algorithm; paper on product submitted	Uncertainty estimated over widely distributed times / location by multiple investigators; Differences understood	Data and source code archived and publicly available; uncertainty estimates provided; known issues public	May be used in applications; assessments have demonstrated positive value
Operational	5	Minimal code changes expected; stable, portable and reproducible	Complete at collection level. Stable. Allows provenance tracking and reproducibility of dataset. Meets international standards for dataset	Public ATBD, Review version of ADD and PG, peer-reviewed publications on algorithm and product	Consistent uncertainties estimated over most environmental conditions by multiple investigators	Record is archived and available with associated uncertainty estimate; known issues public. Periodically updated	May be used in applications by other investigators; assessments demonstrating positive value
	6	No code changes expected; Stable and reproducible; portable and operationally efficient	Updated and complete at collection level. Stable. Allows provenance tracking and reproducibility of assessment.. Meets current international standards for dataset	Public ATBD, ADD and PG; Multiple peer-reviewed publications on algorithm and product	Observation strategy designed to reveal systematic errors through independent cross-checks, open inspection, and continuous interrogation; quantified errors	Record is publicly available from Long-Term archive; Regularly updated	Used in published applications; may be used by industry; assessments demonstrating positive value

Table 1. The Science Algorithms to Operations (SATO) Product Maturity Matrix for Landsat science products, adopted and modified from the NOAA Climate Data Record (CDR) maturity model (Bates & Privette, 2012).

170

The progression and transformation of the product follow a structured procedure, with milestones and responsibilities agreed on between the USGS Landsat science project and the algorithm principal investigator(s). Work is divided into a series of sequential phases, as follows:

Research Stage (Maturity Levels 1 and 2): During this stage, academic researchers and principal investigators lead the process. The product remains publicly restricted until it is published, because significant changes to the source code are expected. Meanwhile, principal investigators submit peer-reviewed journal articles describing the algorithmic approach.

Provisional Stage (Maturity Levels 3 and 4): Research and development entities, such as USGS EROS, lead and optimize the execution of the algorithm. A provisional version of the product becomes publicly available on-demand. Source code modifications continue, and metadata, documentation, and the Algorithm Description Document (ADD) and Product Guide (PG) are published along with the provisional product package. Algorithm uncertainties are estimated, and product limitations are documented.

Operational Stage (Maturity Levels 5 and 6): Operational entities, like the USGS EROS Data Processing and Archive System (DPAS), lead this stage. The algorithm is ported into an operational environment and publicly distributed for operational applications. It is stable, reproducible, and its provenance is recorded in standardized metadata. Peer-reviewed validation methods and published algorithms ensure reliability. Known issues and uncertainties are transparently disclosed.

Throughout a product's provisional lifetime, modifications to its features are expected, although the underlying algorithm to generate the product (e.g., aquatic reflectance) is unchanged. For example, algorithm ingestion into ESPA often involves modifying source code for greater processing efficiency as well as for reproducibility. Science verification at each step is conducted to ensure no anomalies are detected in the data and that any alterations or updates to the source code do not have a direct impact on the algorithm itself. Metadata standards are used to ensure product attributes are an accurate representation of the data, are understandable, and can be referenced. After verification and quality checks, the data product is released through the ESPA on-demand interface for public availability along with documentation and any known caveats published on the USGS product web page. Provisional data products are generated to enable timely scientific use and garner user feedback on quality, algorithm performance, observed uncertainties over diverse geographical regions, and community validation following early adopter feedback. It is the responsibility of USGS EROS to compile this information from the community, work with corresponding research groups, and routinely assess other candidate algorithms with potential principal investigators.

3 Key Takeaways

Since their release to the public in 2020, order requests for the Landsat 8/9 Level 2 provisional AR products from ESPA by the community have now surpassed 90,000 scene downloads as of the end of September 30th, 2024 (Fig. 2). Maximum downloads were observed during the first year of release (and the re-release, following the availability of Collection 2), followed by downward trends with each passing fiscal year. The release of Landsat 8/9 provisional AR products allowed the opportunity to gain insights from the scientific user community on the quality and accuracy of the products. Examples of product feedback include research articles and agency reports that evaluate provisional Landsat AR products across a variety

of aquatic scientific applications, including coastal ocean color mapping (Nazeer et al., 2020; Tavora et al., 2023), lake water quality monitoring (Ogashawara et al., 2020; Niroumand-Jadidi, et al., 2022), and satellite-derived bathymetry (Poppenga & Danielson, 2021).
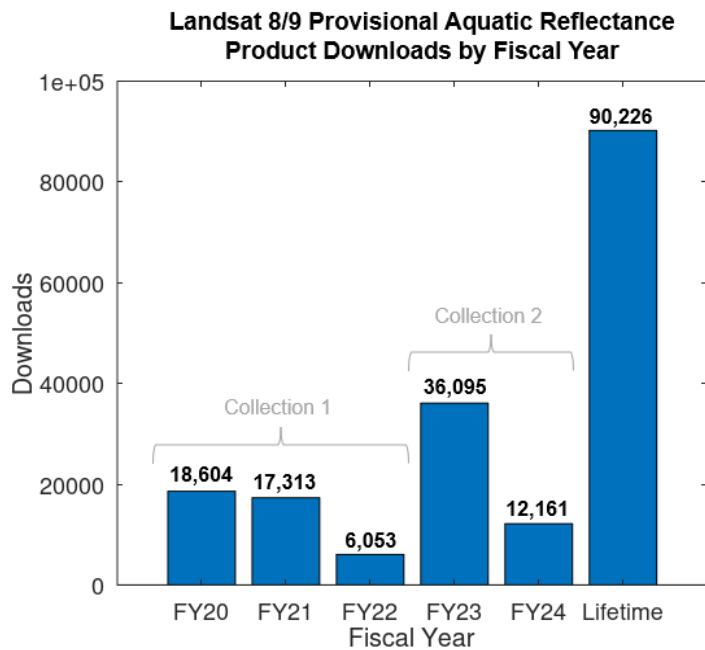
210

Figure 2. Annual download metrics of the Landsat 8/9 provisional AR science products. While not formally part of a Collection themselves, the AR products have been released using either Collection 1 or Collection 2 input data.

Landsat 8/9 provisional AR product limitations were recognized by the scientific community concerning (1) the omission of valid water pixels associated with the l2gen-based land/water delineation and (2) negative AR values generated primarily over inland and optically complex coastal waters (Pahlevan et al., 2019; Ilori et al., 2019; Ogashawara et al., 2020; Tavora et al., 2023). While a new water masking approach was developed for the re-release of the provisional products associated with Collection 2 to mitigate the inconsistencies associated with the l2gen-based land/water delineation, the negative values resulting from atmospheric correction remain a challenge that has been well documented in the literature across a suite of ocean colour applications (Ruddick et al., 2000; Melin et al., 2011; Bramich et al., 2018; Wei et al., 2018; Kuhn et al., 2019; Pahlevan et al., 2021). Negative AR, which can significantly affect the accuracy of downstream water quality products, has been primarily attributed to the challenges of utilizing one or more NIR spectral bands to characterize aerosol path radiance(s) (L_a) over highly turbid or productive, complex case-2 type waters (Bailey et al., 2010; Werdell et al., 2010; Dash et al., 2012; Ibrahim et al., 2019; Wang et al., 2022). In these optically challenging water bodies, the traditional assumption that water-leaving radiance in the NIR portion of the electromagnetic spectrum is negligible (or effectively estimated by the assumptions

of the algorithm) is not valid. Instead, such algorithms may underestimate the substantial water-leaving NIR contribution in highly turbid or productive waters, leading to overestimation of L_a and, consequently, dragging the downstream AR to low and even negative values (Fig. 3). This issue is intensified for inland freshwater systems, which contain varying amounts of coloured dissolved organic matter, suspended sediments, phytoplankton, and surrounding land pixels bordering the entire lake shoreline. Accurate aerosol correction in such environments is crucial for reliable water quality assessments, and addressing these limitations will be decisive for the success of Landsat AR products in future Collections. Other challenges faced by SeaDAS (and many other algorithms designed for ocean colour) include factors such as mitigating sun glint and a missing correction for adjacency effects. Increasing user awareness of these issues may explain the observed downward trend in USGS provisional AR product downloads over time. In response, the provisional product package updates that followed the release of Landsat Collection 2 also augmented the suite of data layers to include AR for the NIR band, per-pixel angle bands, intermediate auxiliary input data and Rayleigh-corrected reflectance products so that users would have supplementary information to further investigate instances when and where full atmospheric correction fails (Table 2). However, these issues must be more fully addressed for the AR product to reach operational maturity. Concurrently, comprehensive aquatic-based atmospheric correction research and applications published by a variety of authors and institutions have provided alternative approaches that may be better suited to compensate for aerosols in the atmosphere over complex water targets (Steinmetz et al, 2011; Brockmann et al., 2016; Moses et al., 2017; De Keukelaere et al., 2018; Vanhellemont, 2019); consequently, some users could be performing their own processing on Level-1 Landsat data using these alternative approaches rather than relying on the provisional AR products from USGS EROS.
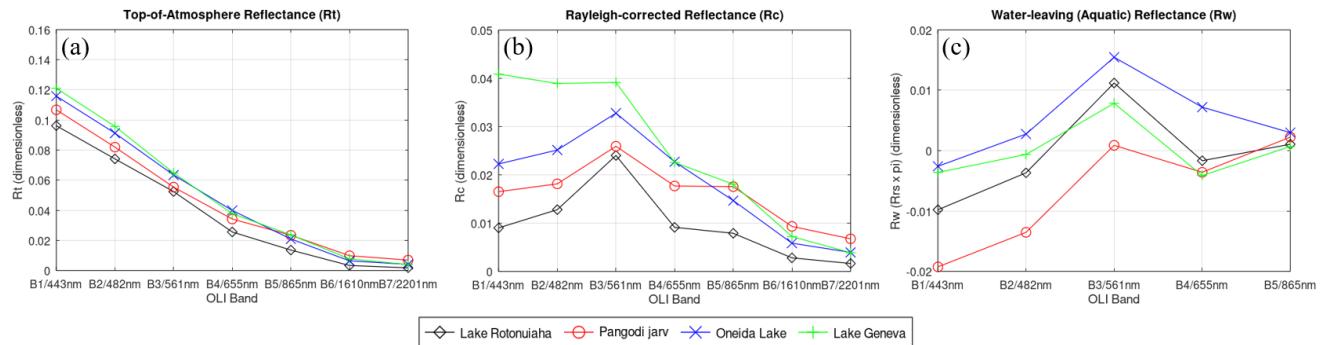
Figure 3. Examples of Landsat 8 top-of-atmosphere (TOA) reflectance (a), Rayleigh-corrected reflectance (b), and Landsat 8 provisional aquatic reflectance (AR= $Rrs * \pi$) (c) for a collection of freshwater bodies, including Lake Rotonuiaha, New Zealand on December 11th, 2017 (LC08_L1TP_072087_20171211_20200902_02_T1), Pangodi järv, Estonia on May 26th, 2018 (LC08_L1TP_187019_20180526_20200901_02_T1), Oneida Lake, New York, USA on August 30th, 2014 (LC08_L1TP_015030_20140830_20200911_02_T1), and Lake Geneva, Switzerland on April 12th, 2020 (LC08_L1TP_196027_20200412_20200822_02_T1). Atmospheric interference impacts the spectral profile retrieved by the sensor in low Earth orbit, obscuring key reflectance and absorption features of the optically active constituents in surface waters (a). The Rayleigh

correction mitigates the molecular scattering contribution from atmospheric gases, allowing for the retrieval of representative spectral profiles of diverse water targets (b). However, overcorrection of aerosols can lead to negative provisional AR spectra in the VIS bands (c).

Description	Band Name	Unit
Aquatic Reflectance Bands 1-4 (VIS)	AR_BAND (1-4)	Unitless
Aquatic Reflectance Band 5 (NIR)*	AR_BAND5	Unitless
Rayleigh-Corrected Reflectance Bands 1-7 (VSWIR)*	RHORC_BAND(1-7)	Unitless
Elevation*	HEIGHT	Meters
Vertical Columnar Ozone (O$_3$)*	OZONE	Dobson Unit
Water Vapor*	WATER_VAPOR	g/cm^2
Surface Pressure*	PRESSURE	Millibars
Wind Speed*	WINDSPEED	m/s
Tropospheric NO$_2$*	NO2_TROPO	10^{15} molecules/ cm^2
Scattering Angle*	SCATTANG	Degrees
Processing Flags	L2_FLAGS	N/A
Water Mask*	WATER_MASK	N/A
Level 1 Pixel Quality Assessment	QA_PIXEL	Bit Index
Level 1 Solar Zenith Angle*	SZA	Degrees
Level 1 Solar Azimuth Angle*	SAA	Degrees
Level 1 Viewing Zenith Angle*	VZA	Degrees
Level 1 Viewing Azimuth Angle*	VAA	Degrees
Level 2 XML Metadata file	.xml/.MTL	N/A

255

Table 2. Landsat 8/9 provisional AR product package contents. Items marked with an asterisk were added following the release of Collection 2. Downloads are delivered inside of a .tar file, in a compressed zip file (tar.gz) named in a similar fashion to other Landsat products available from ESPA. Additional specifications and attributes for these files can be found in Section 3 of the Landsat 8/9 provisional Aquatic Reflectance Product Guide (USGS, 2025).

4 Research Methods

4.1 Toward reliable validation of Landsat aquatic reflectance

The USGS EROS SATO maturity matrix requires uncertainty estimates of varying sophistication at different product maturity levels. In practice, rigorous estimates of uncertainty are difficult to achieve and assessments of the quality of the product suite instead rely on comparisons of satellite data with *in situ* measurements. Limitations on the ability to validate the in-development Landsat 8/9 AR products have contributed to these data remaining in the provisional stage. Indeed, finding a

collection of reliable validation datasets that represents the full spectrum of optical variability of inland waters observable by Landsat has been challenging. Previous validation efforts for aquatic based atmospheric correction processors over surface waters in the optical domain have relied heavily on NASA's Ocean Color component of the Aerosol Robotic Network (AERONET-OC) (Wei et al., 2023) and historical field data records from community-made observations (Pahlevan et al., 2021; Lehmann et al., 2023). Close agreement between satellite and *in situ* data is widely recognized within the aquatic community as necessary for ensuring the quality of a remote sensing-based product (Ogashawara et al., 2024)

The AERONET-OC Data Display Interface provides access to normalized water-leaving radiances (nL_w) collected in various wavebands by platform-based spectroradiometers across a network of coastal and select inland water bodies. These data are frequently used for vicarious calibration and validation exercises for global ocean colour missions (Zibordi, et al., 2006; Zibordi et al., 2009). The ongoing radiometric measurements collected from AERONET-OC platforms, using calibrated CE-318 sun photometers (Johnson et al., 2022), combined with the systematic Landsat 8/9 multispectral acquisitions, provide frequent matchups (near-coincident observations) that allow the scientific community to evaluate Landsat AR algorithm outputs (Mao et al., 2013; Vanhellemont et al., 2014; Bassani et al., 2016; Mannino et al., 2016; Ilori et al., 2019; Xu et al., 2020; Yan et al., 2023; Arena et al., 2024). Preliminary intercomparison exercises between Landsat 8/9 with AERONET R_{rs} data have been used to showcase the fidelity of Landsat to derive AR measurements that are comparable to those of preceding global ocean colour missions. However, the locations of the platforms are generally biased toward representing moderately turbid (e.g., 0.3 < total suspended solids [TSS, g m-3] < 1.2 & 0.5 < chlorophyll a [Chl-a, mg m-3] < 2.0) coastal and open ocean waters (Pahlevan et al., 2021). The limited number of inland platforms sit on sizeable freshwater bodies within the United States which include Lake Okeechobee, FL (~1,740 km2); Lake Erie, OH (~25,700 km2); and south Green Bay, WI (~1,360 km2) so that freshwater studies can be conducted with operational ocean colour sensors. These inland water bodies experience highly productive seasonal cyanobacterial blooms, so the platforms are essential for understanding the relationships between chlorophyll concentrations and radiometry with respect to satellite observations (Lekki et al., 2019; Moore et al., 2019). However, these freshwater systems do not adequately represent the full spectrum of optical variability of inland waters observed by Landsat across the globe (Pahlevan et al., 2018).

The GLObal Reflectance community dataset for Imaging and optical sensing of Aquatic environments (GLORIA) was released in 2022 (Lehmann et al., 2023). This collection of 7,572 curated proximal hyperspectral remote sensing measurements from 450 different water bodies worldwide was contributed by researchers across 53 institutions. The R_{rs} data are provided at a resampled 1 nm spectral interval within the 350 to 900 nm wavelength range and are complemented with several co-located water quality variables (Chl-a, TSS, coloured dissolved organic matter [CDOM]) as well as instrumentation and measurement procedures. Environmental conditions at the time of data acquisition (sky conditions, windspeed, surrounding land cover, etc.) are also included. The authors have considered the dataset the "de facto state of knowledge" of *in situ* coastal and inland aquatic optical diversity and thus may provide a validation record for the inland waters that is complementary to freshwater

AERONET data. Together, these datasets could help provide insight into the general accuracy of the Landsat provisional AR products and support the progress of Landsat AR research and development toward the operational phase.

4.2 Validation methodology

Landsat 8/9 OLI acquisitions with accompanying same-day *in situ* measurements across the combined AERONET-OC and
305 GLORIA datasets were identified to generate a radiometric validation record (Crawford et al., 2025[1]). From the 7000+ available GLORIA R_{rs} measurements between 2013 (launch of Landsat 8) and 2022 (end of GLORIA record), 1,794 were coincident within +/- five days of Landsat 8/9 acquisitions. To minimize the influence of rapid changes in surface water conditions while preserving a statistically robust number of matchups, the temporal window for satellite and *in situ* data collocation was constrained to within ±3 hours. This approach aligns with established validation protocols that emphasize the
310 trade-off between temporal proximity and sample size in matchup analyses (Concha et al., 2021). GLORIA R_{rs} spectra were then screened using the Quality Water Index Polynomial (QWIP) and only selecting samples that fell within -0.2 and 0.2 (Dierssen et al., 2022). Finally, clear water Landsat pixels were selected as classified by the corresponding pixel quality assessment layer (QA_PIXEL) as unobscured (no cloud or cloud shadow) water (Fmask 3.3.1, Zhu et al., 2015; Crawford et al., 2023). This screening process resulted in a total of 554 matchups between GLORIA and Landsat 8/9, resulting in 481 of
315 samples representing freshwater lakes, 45 matchups representing the coastal ocean waters, 12 samples classified as rivers, 13 as estuary, and 3 considered as "other". Corresponding labels of water type for all matchups were subjectively assigned (e.g., "sediment dominated", "chlorophyll dominated", "clear") by the sample collector as established by the co-located water quality parameter concentration (Chl-a, TSS, CDOM).

320

Figure 4. Global distribution of the combined AERONET-OC ($n_{aeronet}$=418) and GLORIA (n_{gloria}=554) matchups with Landsat 8/9 acquisitions.
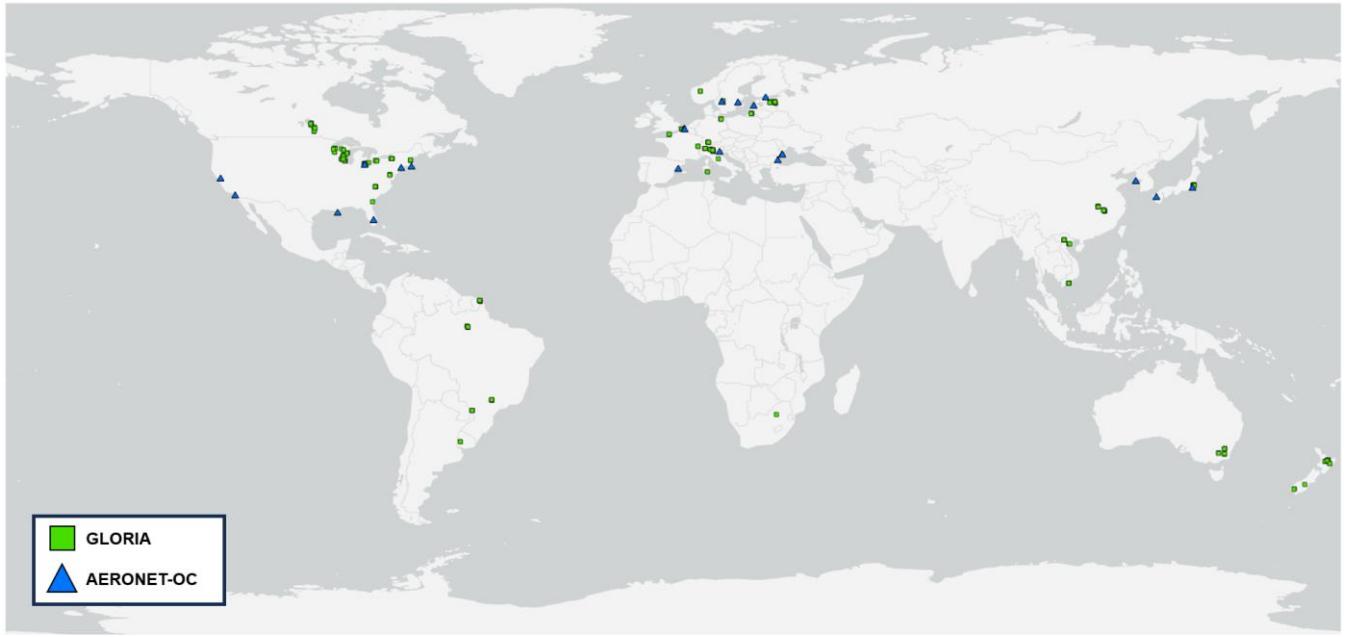
Following a similar approach, 418 AERONET-OC records ($n_{aeronet}$) were found to match up with 412 same-day OLI
325   acquisitions using the same QA_PIXEL cloud filter and temporal window criteria. Level 1.5 AERONET-OC normalized water-leaving radiance nL_w data were selected to increase the number of available OLI acquisitions per site, despite a potentially lower accuracy than the Level 2 products that may involve a final calibration procedure (Pellegrino et al., 2023). After retrieving nL_w from the AERONET-OC database, R_{rs} was subsequently calculated for each sample:

$$R_{rs}(aeronet) = \frac{nL_w(\lambda)}{F_0(\lambda)} (sr^{-1}), \qquad (5)$$

330   where F_0 is the extraterrestrial solar irradiance which has been obtained from the Total and Spectral Solar Irradiance Sensor (Coddington et al., 2021) model and then spectrally convolved with the spectral response function of the corresponding Landsat 8/9 OLI sensor. For both GLORIA and AERONET-OC datasets, no spectral resampling was applied. Instead, R_{rs} values were extracted at wavelengths closest to the Landsat OLI band centers (443nm, 482nm, 561nm, and 655nm). This nearest-band approach avoids potential uncertainties introduced by spectral convolution, which can be sensitive to the spectral shape of the
335   *in situ* data and the accuracy of the sensor's spectral response functions.

Following the data extraction technique of Pahlevan et al. (2021), average R_{rs} pixel values from a 5x5 window centered on AERONET-OC site were retrieved from the coincident provisional Landsat AR products. To mitigate potential spectral contamination from the platform, the middle 3x3 window of pixels was discarded. For GLORIA matchups, the average pixel

values from a 3x3 window centered on the GLORIA sample location were retrieved. Accuracy assessment was conducted on a per-band basis and employed fundamental statistical metrics often used in ocean colour radiometry (Seegers et al., 2018; Pahlevan et al., 2021; Wei et al., 2025) to evaluate the performance and reliability of the Landsat 8/9 Level 2 provisional AR products. The median symmetric accuracy (ε) was calculated to express the relative accuracy as a percentage, enabling comparisons with those relevant across the aquatic remote sensing community:

$$\varepsilon\ (\%) = 100 \times \left(exp\left(median\left(\left|Ln\left(\frac{Rrs_{OLI}(\lambda)}{Rrs_{in\ situ}(\lambda)}\right)\right|\right)\right) - 1\right), \tag{6}$$

Additionally, the signed symmetric bias metric (β) was incorporated to identify any systematic errors, which determines whether provisional AR products are overestimating or underestimating *in situ* values:

$$\beta\ (\%) = 100 \times median\left(Ln\left(\frac{Rrs_{OLI}(\lambda)}{Rrs_{in\ situ}(\lambda)}\right)\right), \tag{7}$$

Finally, the mean absolute difference (MAD) was used to quantify the average magnitude of error between each Landsat 8/9 provisional AR VNIR spectral band and its corresponding band in both AERONET-OC and GLORIA *in situ* validation dataset, providing an estimate of the typical uncertainty in the geophysical parameter being measured:

$$MAD = \frac{1}{n}\sum_{i=1}^{n} |Rrs_{in\ situ}(\lambda) - Rrs_{OLI}(\lambda)|, \tag{8}$$

The AERONET-OC validation dataset benefits from internal consistency due to standardized protocols and calibrated CE-318 sun photometer measurements for retrieving water-leaving radiance. In contrast, the GLORIA dataset's variability warrants caution if it is to be used as a routine reference for validation purposes (Wei et al., 2025). This variability stems from the diversity of contributors and collection methods (Fig. 5). With data contributions from 20 different organizations, the collection process is subject to differences in protocols, standards, and expertise. Frequent cloud cover, haze, sun glint effects, and unfavourable environmental conditions (e.g., high winds) provide further challenges and diminish validation opportunities, particularly in low and high latitudes (Radeloff et al., 2024). Although environmental conditions and measurement method were documented for each sample collected (12 different measurement methods total), the inclusion of 18 known radiometer instruments further complicates consistency, because each instrument has varying levels of calibration, accuracy, and uncertainty.
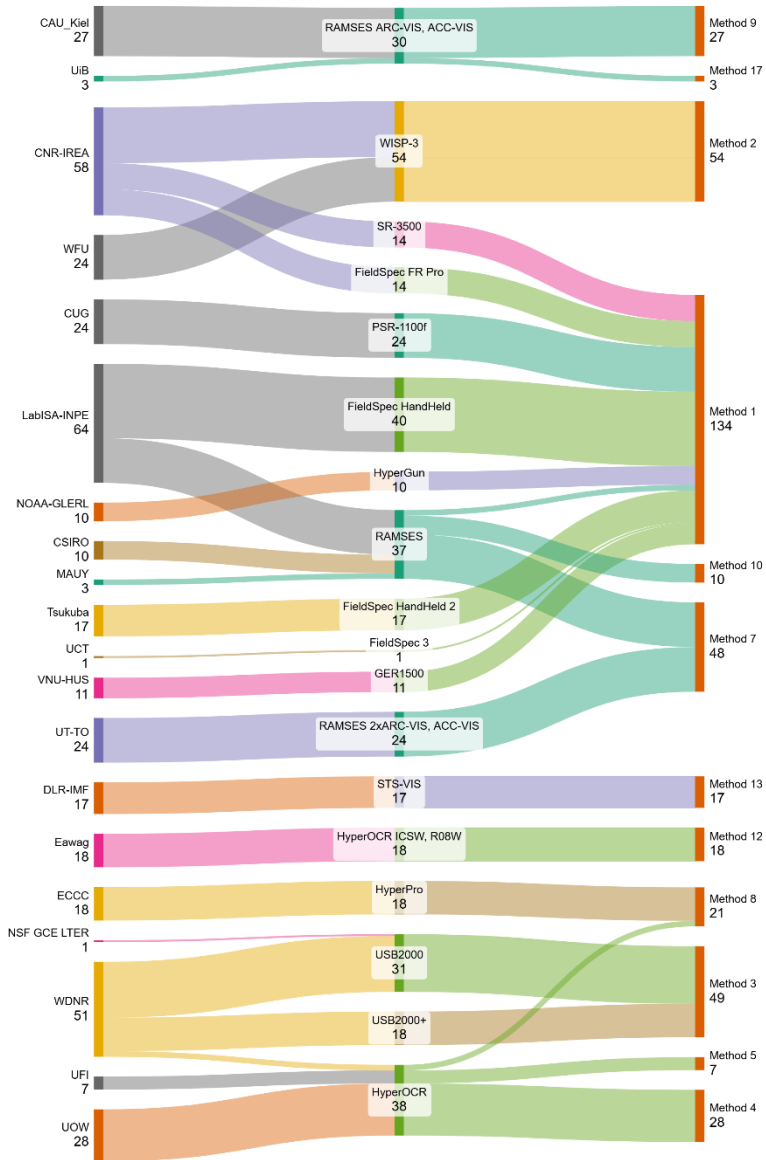
Figure 5. Sankey diagram capturing the methodological variability of GLORIA *in situ* R_{rs} data across contributing institutions. Valid matchup sample distribution includes contributions from 20 different organizations, using 18 known radiometer instruments, practicing 12 different radiometric measurement methods (refer to Table A.1 and A.2 in the appendix for method descriptions and organization acronym definitions).

The Global Climate Observing System (GCOS) scientific community has established threshold (T), breakthrough (B) and goal (G) targets values of uncertainty for satellite-derived water-leaving reflectance products to be met to ensure that data are useful (GCOS 2025). While the established GCOS values are not a standard requirement for Landsat Level-2 operational production,

the observed ε between satellite and *in situ* measurements are used as a stand-in for the GCOS 2-sigma uncertainty metric in this study, which has a threshold requirement of 30%.

5.0 Results

The performance of the Landsat 8/9 Collection 2 Level 2 provisional AR R_{rs} products was evaluated using *in situ* R_{rs} measurements from AERONET-OC ($n_{aeronet} = 418$) and GLORIA ($n_{gloria} = 554$) matchups against a selection of comparison metrics described in Section 4.2. For the AERONET-OC subset, the AR products exhibited strong agreement with AERONET-OC observations. MAD values were low across all bands, ranging from 0.0006 sr⁻¹ in the red band to 0.0014 sr⁻¹ in the coastal band (Fig. 6/Table 3). Median symmetric accuracy (ε) was below the GCOS 30% threshold in the blue (27.6%) and green (19.8%) bands, while the coastal (40.7%) and red (33.0%) bands slightly exceeded this limit. Signed symmetric bias (β) indicated a tendency toward underestimation of the AR products in B1–B3, with the strongest bias observed in the coastal band (–23.1%). The red band (B4) showed a slight overestimation (β = 6.6%). In contrast, comparisons with GLORIA revealed substantially higher variation. MAD values ranged from 0.0046 sr⁻¹ (B4) to 0.0064 sr⁻¹ (B1). Values of ε exceeded the GCOS threshold in all bands, ranging from 39.6% (green) to 68.4% (coastal). Values of β were strongly negative across all bands (–36.8% to –62.0%), indicating consistent underestimation of reflectance values by the AR products relative to GLORIA observations. This generally follows the wavelength trends in the l2gen performance for the OLI sensor seen in the aquatic component of the atmospheric correction intercomparison exercise (ACIX-Aqua) (Pahlevan et al., 2021). The larger MADs seen with the GLORIA comparisons are in part due to the higher frequency of negative values in the provisional AR products over GLORIA-sampled locations. The combined dataset yielded intermediate results. MAD values ranged from 0.0028 sr⁻¹ (B4) to 0.0042 sr⁻¹ (B1). The ε values exceeded the 30% threshold in all bands except green (29.3%), with values ranging from 35.0% (red) to 49.9% (coastal). The β values remained negative across all bands, with the strongest underestimation in the coastal band (–39.8%) and the weakest in the red band (–19.9%).
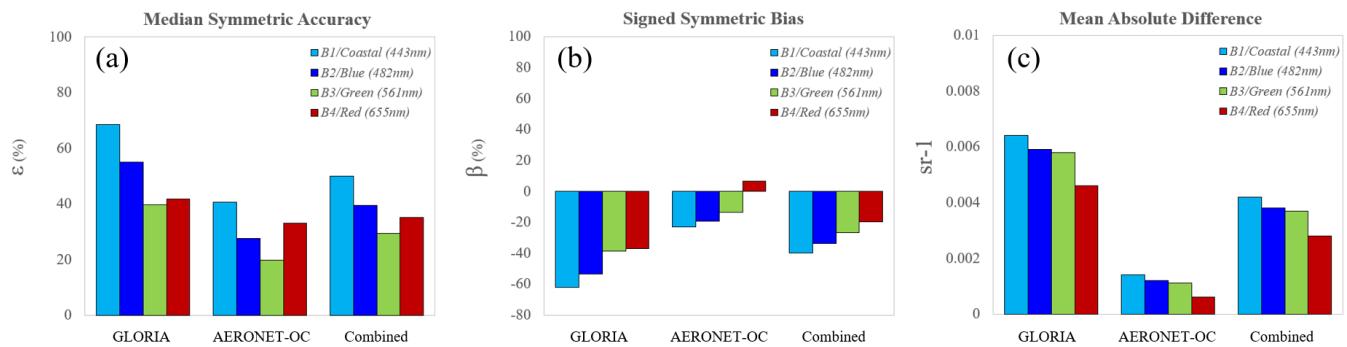
Figure 6. Performance metrics used to evaluate the accuracy of Landsat 8/9 provisional AR products between AERONET ($n_{aeronet} = 418$), GLORIA ($n_{gloria} = 554$), and the combined ($n_{combined} = 972$) R_{rs} matchup datasets.

The per-band scatter plots shown in Figure (7) provide a closer look into the spread of OLI derived AR R_{rs} between each of the AERONET-OC and the GLORIA matchup datasets. Most notably, when evaluated against AERONET-OC data, the AR products demonstrated strong linear agreement, particularly in the green ($R^2 = 0.89$) and red ($R^2 = 0.91$) bands (Table 3). Moderate correlations were observed in the blue ($R^2 = 0.76$) and coastal ($R^2 = 0.57$) bands, suggesting that the AR products are generally reliable in optically simple environments. In contrast, comparisons with GLORIA revealed very weak correlations across all bands, with R^2 values ranging from 0.06 (B1) to 0.29 (B4), primarily due to the substantial amount of negative AR values. The combined dataset reflected this discrepancy, with low R^2 values across all bands (0.06–0.35), further emphasizing the limited predictive strength of the AR products in more complex or variable aquatic environments.
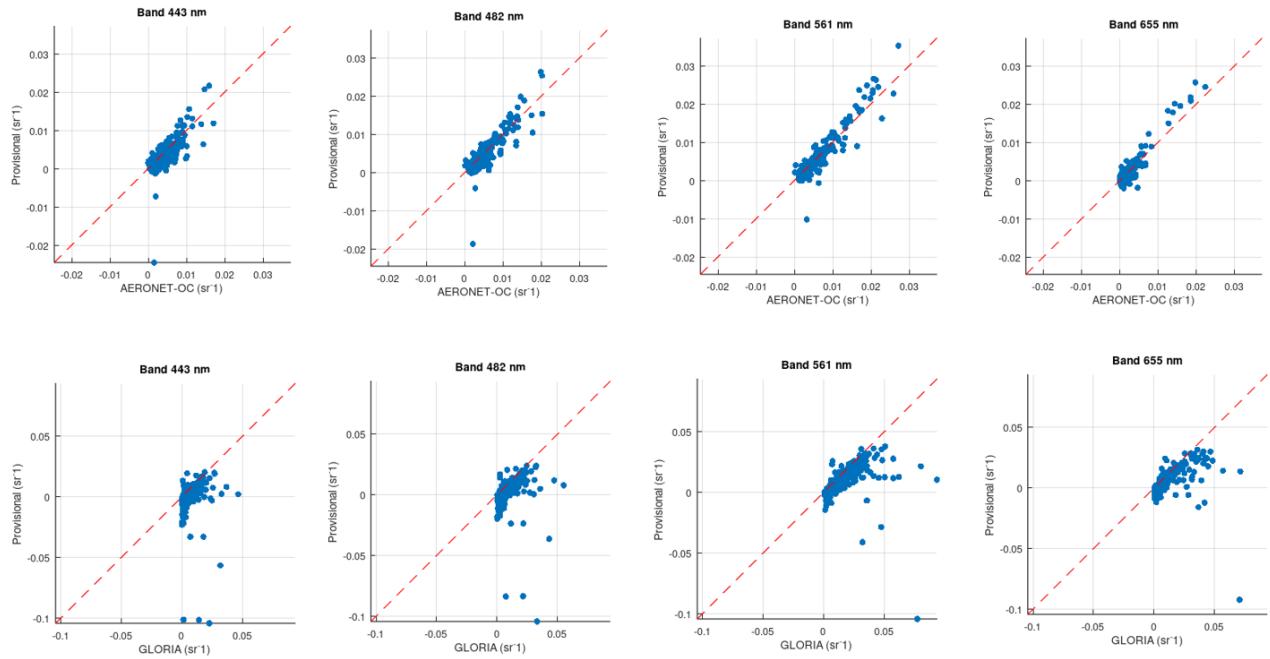
Figure 7. Per band scatter plots between Landsat 8/9 provisional AR with AERONET-OC (top) and GLORIA (bottom) *in situ* R_{rs} matchups. 1:1 line shown in red.

Dataset	OLI Band	MAD (sr⁻¹)	ε (%)	β	R²
AERONET-OC (n=418)					
	B1/Coastal/443nm	0.0014	40.7	-23.1	0.57
	B2/Blue/482nm	0.0012	27.6	-19.1	0.76
	B3/Green/561nm	0.0011	19.8	-13.4	0.89

	B4/Red/655nm	0.0006	33.0	6.6	0.91
GLORIA (n=554)					
	B1/Coastal/443nm	0.0064	68.4	-62.0	0.06
	B2/Blue/482nm	0.0059	54.9	-53.2	0.09
	B3/Green/561nm	0.0058	39.6	-38.5	0.24
	B4/Red/655nm	0.0046	41.6	-36.8	0.29
COMBINED (n=972)					
	B1/Coastal/443nm	0.0042	49.9	-39.8	0.06
	B2/Blue/482nm	0.0038	39.4	-33.8	0.10
	B3/Green/561nm	0.0037	29.3	-26.6	0.31
	B4/Red/655nm	0.0028	35.0	-19.9	0.35

Table 3. Tabulated values of the per-band accuracy assessment of the Landsat 8/9 Level 2 provisional AR products between AERONET-OC ($n_{aeronet} = 418$) and GLORIA ($n_{gloria} = 554$) R_{rs} matchups.

415

The classification of inland waters into varying optical water types is driven by the biogeochemical properties in the water column. Differences between GLORIA *in situ* R_{rs} and Landsat 8/9 Level 2 provisional AR highlight how these properties influence the sensitivity of the validation assessment. Specifically, the magnitude of the differences, reflected by ε, can vary dramatically across different water types (Fig. 8). This variability indicates that the performance of the Landsat 8/9 provisional
420 AR retrieval is highly context-dependent—errors are minimal in optically simple waters (e.g., clear to moderately turbid coastal waters) but increase considerably in optically complex waters where factors such as elevated levels of turbidity, chlorophyll concentrations, or coloured dissolved organic matter (CDOM) dominate the water column.
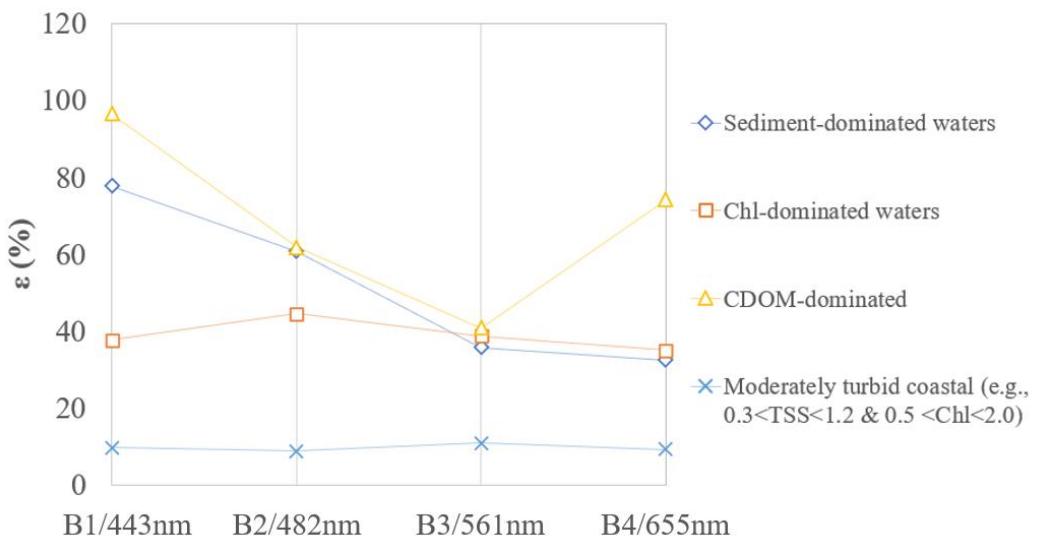
 Figure 8. Isolated median symmetric accuracy (ε) between GLORIA *in situ* R_{rs} and Landsat 8/9 Level 2 provisional AR by reported water type.

6 Discussion

6.1 Recent advancements in aquatic reflectance retrieval

Aquatic reflectance represents a particular challenge for the Landsat project, with its emphasis on long-term monitoring, because the performance of heritage Landsat sensors is marginal with respect to the needs of aquatic science (Pahlevan & Schott, 2012; Schott et al., 2016). Improvements in the signal-to-noise ratio (SNR) and radiometric resolution of the Landsat 8 OLI sensor spurred the development of the provisional aquatic reflectance product; however, the results of both the internal evaluation described above and other external evaluations (e.g., Ogashawara et al., 2020) suggest that further re-evaluation of the algorithmic approach and introspection of the consistency of *in situ* datasets are warranted. The state of the field of atmospheric correction over water remains fluid, and new approaches and refinements to existing approaches have arisen since USGS began its SATO process for aquatic reflectance. In this section, we briefly review the major directions of research pertaining to atmospheric correction over water.

We broadly classify aquatic reflectance processors based on the major assumptions or characteristics of their approach, as follows: (a) corrections based on a variant of the "black pixel" assumption, (b) spectral ratios and spectral shape matching, (c) machine-learning assisted inversion of forward radiative transfer modelling, and (d) over land atmospheric correction for surface reflectance adapted to additionally retrieve aquatic reflectance.

The "black pixel" approaches to estimating the aerosol contribution are well-known in remote sensing literature and rely on an assumption that water-leaving radiance is negligible/correctable in at least one (if an aerosol model is known or assumed) or two (if an aerosol model is to be selected) bands. For Landsat 8/9, we have already described the implementation of an l2gen-based provisional algorithm, which relies on a pairing of the NIR and SWIR bands to estimate aerosol radiance. This choice arises in part from the lack of a second NIR band on Landsat OLI; the traditional ocean colour remote sensing approach involves two bands in the 700–900 nm range (Wang & Gordon, 2018). Other approaches exist that select SWIR bands (Werdell et al., 2010; Vanhellemont & Ruddick, 2015; He and Chen, 2014) or even a deep blue band (He et al., 2012). A more dynamic approach taken by the "dark spectrum fitting" (DSF) algorithm implemented within the ACOLITE processor allows potentially any band to contribute to the aerosol retrieval (Vanhellemont 2019, Vanhellemont & Ruddick 2018). The key motivation in many of these variants is to address the violation of the core assumption of negligible NIR water-leaving radiance for specific optical water types. Due to the widespread use and high heritage of black pixel-based algorithms, they can often be found within well-maintained software packages with cross-mission support.

Other algorithms rely on assumptions surrounding spectral relationships of the radiometric quantities contributing to the signal. These relationships may be formulated on a theoretical basis, based on the absorptive properties of water, or modeled empirically across a range of water compositions. The bio-optical model that functions as a sub-component of l2gen relies on empirically derived relationships across the visible wavelengths to support iterative $R_{rs}(NIR)$ estimation (Bailey et al., 2010). An approach by Ruddick et al. (2000) relies on the relative invariance of the shape of water-leaving reflectance in the 700–900 nm near-infrared portion of the spectrum to estimate the aerosol contribution over turbid waters. Other approaches (e.g., Singh & Shanmugam, 2014) have been proposed that make use of multiple band ratios and other spectral relationships across multiple wavelengths to disentangle the spectral variability of aerosols. Finally, a more band agnostic approach to atmospheric correction is taken by the POLYMER processor; developed with a focus on addressing sun glint contamination, it makes use of spectral matching against all available spectral bands (Steinmetz et al. 2011; Steinmetz & Ramon, 2018).

Machine learning algorithms provide a mechanism for more general assumptions on spectral relationships that are internalized by a neural network during the training process. These models are trained on the output of radiative transfer simulations that are parameterized across a range of water constituents, atmospheric conditions, and observational characteristics. In-situ bio-optical or radiometric databases aid in developing realistic parameterizations. For example, the Case 2 Regional Coast Colour (C2RCC; Brockmann et al., 2016) processor encompasses separate sets of neural nets, each trained over different ranges of optical parameters derived from the NASA bio-Optical Marine Algorithm Data set (NOMAD; Werdell & Bailey, 2005). The Ocean Color – Simultaneous Marine and Aerosol Retrieval Tool (OC-SMART; Fan et al., 2021) is parameterized from MODIS Aqua Level 3 products to estimate reasonable distributions of aerosol and water optical properties. An approach based on mixture density networks (MDNs) has been implemented in the AQUAVERSE (AQUAtic inVERSion schEme for remote sensing of fresh and coastal waters; Ashapure et al., 2025) framework, although as the time of this publication, this processor is too new to have been included in formal intercomparison exercises.

A final set of approaches involve leveraging terrestrial surface reflectance algorithms to constrain the aerosol properties and generate aquatic reflectance by correcting the over-water surface reflectance for sun and sky glint. This has been demonstrated within the iCOR processor (De Keukelaere et al., 2018), which showed good performance in match-up intercomparisons (Pahlevan et al., 2021). This manner of approach provides a considerable reduction in complexity by reducing the number of algorithms that must be maintained. However, these algorithms rely on scene content that might be sparse or absent for some over-water footprints; as such, the performance in such areas would depend on the fidelity of the algorithm's internal fallback approach. Other approaches include those that offer a consistent framework that can be applied to retrieve surface or aquatic reflectance (e.g., Thompson et al., 2019).

The differences between the above algorithms predominantly focus on atmospheric characterization, but other radiometric components have been highlighted within the research community as outstanding concerns. Sun glint and adjacency effects

are two such issues. Some atmospheric correction processors include a correction for one or both; however, at the level of algorithm intercomparison exercises, sun glint and adjacency effect components are not typically evaluated separately. Landsat does not have the anti-sunward tilt that many ocean colour sensors use to avoid high glint risk geometries; as such, pixels from certain observations (particularly those acquired at lower latitudes) will suffer from glint contamination. Scattered light from

495   nearby landmasses or clouds provides excess signal to darker water bodies that can interact with algorithms in complex ways (Wu et al., 2024). Providing users with detailed quality information at the pixel level to enable users to filter out potentially problematic data is one mitigating strategy (e.g., CEOS, 2022) but research to better characterize and remove these contributions will further improve data utility.

6.2 Considerations for Landsat algorithm adoption

500   USGS continuously evaluates the state of the field for maturing science algorithms relevant to its Level 2 science product goals. Key criteria that are considered when evaluating external algorithms include (1) a robust presence in the scientific literature, including intercomparison exercises; (2) global applicability across a broad range of environmental and observational conditions; (3) ability to maintain consistency across the Landsat historical record; (4) support for multiple Landsat sensor generations; (5) free, open source algorithm code for which only moderate further development is required;

505   and (6) ability of the code to run at operational scales within reasonable budgetary constraints, after optimization.

Criteria 1–2 are meant to promote algorithms that are well-supported by evidence and have garnered interest within the research community. With a few exceptions, the algorithms mentioned in the previous section are found in one of several published algorithm intercomparisons such as the second Atmospheric Correction Intercomparison eXercise (ACIX-II or ACIX-Aqua;

510   Pahlevan et al., 2021) or the report (in draft form at the time of this writing) by the International Ocean Colour Coordinating Group (IOCCG; Bailey et al., 2024) regarding atmospheric correction over turbid waters. ACIX-Aqua, jointly organized by NASA and ESA, focused on aquatic retrievals over coastal and inland waters for Landsat 8 and Sentinel-2. In this regard it is more directly relevant than the IOCCG (2019) report, for which the evaluations were performed against MODIS Aqua data. Because Landsat Collection processing is meant to support diverse applications, algorithms must be applicable across a broad

515   range of environmental conditions.

The ACIX exercise indicated that in general, the relative performances of aquatic atmospheric correction processors against *in situ* data from AERONET-OC and a community validation dataset (CVD) depend on optical water type (OWT) to such a degree that a top-performing processor for one OWT was often a low or bottom performer in another, in one or more

520   wavelengths. Pahlevan et al. (2021) suggest that a "fit-for-purpose" solution that reflects the specific downstream needs may be the best supported approach based on the analysis. It is conceivable that a blend of algorithms may offer a compromise solution (e.g., Wang & Shi, 2007; Liu et al., 2019; Joshi & D'Sa, 2020), at the price of a substantial increase in complexity

and risk of introducing spatial artifacts. The IOCCG report similarly found that the most turbid OWT disrupted the algorithm rankings substantially, although in other areas the statistical results seemed less competitive than in the ACIX exercise.

525

Criteria 3–4 reflect the need for algorithms that are robust and flexible, yielding results that are consistent through the historical record. Landsat maintains a high degree of consistency in its heritage spectral bands, even if these are supplemented or adjusted in newer missions, with the expectation that heritage bands should result in a long-term time series that appears seamless across satellite generations. Whether Landsat data pre-dating Landsat 8 are deemed of suitable quality for an operational aquatic

530 reflectance product remains to be determined. However, it is anticipated that an AR product will be desirable from future Landsat missions. This provides an additional challenge as to whether an approach that best leverages current capabilities would also be compatible with future (or previous) missions, or if those data would require a bespoke algorithm. As the capabilities of Landsat satellites evolve, striking a compromise between complexity and maintainability may become a driving consideration.

535

Criteria 5–6 focus on several factors relating to software maturity, scalability, and open science. Software development is a key contribution that USGS EROS provides during the SATO process but algorithm code maturity within the research phase is an important factor in determining whether to advance an algorithm further in the SATO phases. Processing requirements are rarely quantified when evaluating atmospheric correction algorithms, and it remains unclear whether these requirements

540 can be meaningfully assessed across processors that differ in maturity and potential for further optimization. Nevertheless, processing millions of Landsat observations (encompassing petabytes of data; Crawford et al., 2023) incurs substantial cost.

Data Availability

Creator(s): Christopher Crawford, Benjamin Page, Saeed Arab, Gail Schmidt, Chris Barnes, Danika Wellington
Title: Landsat 8-9 Operational Land Imager (OLI) Level 2 Provisional Aquatic Reflectance Products, Collection 2 Validation

545 Subset
Publisher/Repository: U.S. Geological Survey ScienceBase
Persistent Identifier: https://doi.org/10.5066/P14MBBRM
Publication Year: 2025

Conclusions

550 The development of an operational AR product for Landsat, facilitated by SeaDAS open-source code, provided a global AR processing capability for the Landsat user community. The l2gen code within SeaDAS has been the flagship processor for generating AR products for Landsat 8 and Landsat 9 OLI data, it may not be the most optimal solution as a single global

processor for current, heritage (Landsat 4/5 TM Landsat 7 ETM+), and upcoming Landsat missions (Landsat Next) in terms of suitability for emerging science needs that require analysis ready data for both inland and coastal water quality mapping

555   applications. The Landsat 8/9 provisional AR performance has shown promising results in the coastal regions, but its reflectance retrieval limitations for inland waters must be acknowledged. These limitations include challenges related to atmospheric correction processing accuracy and consistency across optically and geographically diverse water conditions. Until *in situ* validation campaigns are conducted on a routine basis with standard operating procedures that are community-endorsed, the combined GLORIA and AERONET-OC datasets offer an interim validation pathway for assessing the

560   operational readiness of aquatic and/or ocean colour processing algorithms and data products Addressing these limitations will be critical for the success of Landsat AR products in future Collections. The USGS Landsat science project approach for Landsat AR algorithm research and development recognizes the importance of the SATO process and collaboration with established aquatic principal investigators. Promoting and maintaining success criteria for a global Landsat Collection 3 AR product while remaining aware of evolving mission specifications for Landsat Next is essential. Key criteria include

565   maintaining consistency across spatial and temporal domains, ensuring interoperability with similar products from other medium-resolution multispectral and imaging spectroscopy missions (e.g., Sentinel-2, Environmental Mapping and Analysis Program [EnMAP], Copernicus Hyperspectral Imaging Mission for the Environment [CHIME]) (Pinnel et al., 2024; Alvarez et al., 2022; Dierssen et al., 2021), and balancing the trade-offs necessary to achieve optimal performance in varying atmospheric and optical water conditions. Looking ahead, the next research steps in preparing for Landsat Collection 3 AR

570   development involves undertaking open science algorithm intercomparisons and quantitative validation that considers heritage missions and Landsat Next science readiness simultaneously. These efforts will provide a foundation for more comprehensive and reliable AR products, ultimately contributing to enhanced understanding and management of aquatic environments globally.

Appendix A

GLORIA Measurement Methods Used During Radiometric Sample Collection

Measurement Method Number	Description
1*	Sequential Lt, Lsky, and Es via a plaque on MP*
2*	Simultaneous Lt, Lsky, and Es on MP*
3*	Lu(0-) and Es on pole connected to a spectrometer via fiber optics from MP* or water edge
4*	Lw(0+) and Es afloat away from MP*
5*	Lu(0-) afloat away from MP*, Es on MP*
6	Lt, Lsky, and Es on MP*
7*	Lt, Lsky, and Es on a frame deployed on MP*
8*	Lu(0-) and Ed(0-) in-water profiling from MP*, Es on MP*

9*	Lu(0-) and Ed(z) units on a depth adjustable bar (measurements at -0.21and -0.67m) on a frame afloat away from MP*, Ed unit lifted above water surface for Es
10*	Lu(0-) and Ed(0-) from winch on MP*, Es on MP*
11	Lt and Es on pole from water edge
12*	Lu(0-) and Ed(0-) autonomous in-water profiling from a fixed platform
13*	Sequential Lt and Es via a plaque, mounted on gimbal stabilized pole from MP*
14	Lu(0-) (and Ed(0-) only for depth information) from in-water profiling from MP*, Es recorded simultaneously from same MP* very close to profiler deployment
15	Lt, Lsky, Es, combined with one Lu unit (aperture at -0.05 to -0.10m) placed on pole
16	Sequential Lu(0-) and Es via a plaque, both measurements using an optical fiber to a black masked perspex tube
17*	Lu(0-) and Ed(z) units on a floating frame (measurements at -0.4 m (Lu) and -0.1 m (Ed)) drifting 10m away from vessel

575

Table A.1. Reference table for Fig (7). Brief descriptions of the 17 measurement methods used by each organization that contributed to the GLORIA dataset. Numbers marked in asterisks are those used in the accuracy assessment. For a more detailed definition for each of the protocols, please see Lehmann et al., 2023.

580

Acronym Definitions for the Organizations that contributed GLORIA

Acronym	Description	Location
CAU_Kiel	Christian-Albrechts-Universität zu Keil	Germany
UiB	Universitat de les Illes Balears	Spain
CNR_IREA	Electromagnetic Sensing of the Environment of the National Research Council of Italy	Italy
WFU	Wake Forest University	USA
CUG	China University of Geosciences	China
LabISA-INPE	Instrumentation Laboratory for Aquatic Systems	Brazil
NOAA-GLERL	National Oceanic and Atmospheric Administration Great Lakes Environmental Research Laboratory	USA
UCT	University of Connecticut	USA
CSIRO	Commonwealth Scientific and Industrial Research Organization	Australia
MAUY	Vessel name	United Kingdom
Tsukuba	University of Tsukuba	Japan
VNU-HUS	Hanoi University of Science	Vietnam

UT-TO	Tartu Observatory of the University of Tartu	Estonia
DLR-IMF	German Aerospace Center Remote Sensing Technology Institute	Germany
Eawag	Swiss Federal Institute of Aquatic Science and Technology	Switzerland
ECCC	Environment and Climate Change Canada	Canada
NSF-GCE LTER	National Science Foundation-Georgia Coastal Ecosystems Long Term Ecological Research Program	USA
WDNR	Wisconsin Department of Natural Resources	USA
UFI	Upstate Freshwater Institute	
UOW	University of Wollongong	Australia

Table A.2. Reference table for Fig (7). Acronym descriptions for the 20 organizations and corresponding country that contributed to the GLORIA R_{rs} dataset used this in this study.

Author Contribution

BP led the manuscript. CC oversees the Landsat science production at EROS and provided USGS guidance and expectations. GS was responsible for the implementation of the provisional aquatic reflectance algorithm into the EROS Science Processing Architecture (ESPA) domain. SA assisted with data extraction and processing. CB provided the insight into the Science Algorithms to Operations (SATO) process. DW provided scientific subject matter experience and assisted with the writing process.

Competing Interests

The authors declare that they have no conflict of interest.

Disclaimer

Any use of trade, firm, or product names is for descriptive purposes only and does not imply endorsement by the U.S. Government. ESTS and KBR, Inc. performed work under contract number 140G0121D001 as part of the USGS Land Satellite Data Systems Research and Development project.

Acknowledgements

We would like to thank USGS colleagues Dr. Keith Loftin of the Kansas Water Science Center and Dr. Victoria Stengel of the Geology, Energy Minerals and Science Center in Texas for their thorough and insightful comments and interpretations of
600   Landsat AR research and developments with respect to the water science domain.

References

Alvarez, A. and Turpie, K. R.: Formulating Aquatic Remote Sensing for the Surface Biology and Geology Mission, J. Sci. Res., GC42D–0733, December, 2022.

Arena, M., Pratolongo, P., Loisel, H., Tran, M. D., Jorge, D. S. F., and Delgado, A. L.: Optical water characterization and
605   atmospheric correction assessment of estuarine and coastal waters around the AERONET-OC Bahia Blanca, Front. Remote Sens., 5, 1305787, doi: 10.3389/frsen.2024.1305787, 2024.

Ashapure, A., Smith, B., O'Shea, R., Maciel, D. A., Saranathan, A., Balasubramanian, S. V., and Zhai, P. W.: Aquaverse: A Machine   Learning-Based   Atmospheric   Correction   Framework   for   Inland   and   Coastal   Waters,   SSRN,
610   doi:10.2139/ssrn.5078832, 2025.

Bailey, S. W., Franz, B. A., and Werdell, P. J.: Estimation of near-infrared water-leaving reflectance for satellite ocean color data processing, Opt. Express, 18, 7521–7527, doi: 10.1364/OE.18.007521, 2010.

Bassani, C., Cazzaniga, I., Manzo, C., Bresciani, M., Braga, F., Giardino, C., and Brando, V.: Atmospheric and adjacency
615   correction   of   Landsat-8   imagery   over   inland   and   coastal   waters   near   Aeronet-OC   sites,   ESA   SP., https://hdl.handle.net/10281/129518, 2016.

Bates, J. J. and Privette, J. L.: A maturity model for assessing the completeness of climate data records, Eos Trans. AGU, 93, 441–441, doi:10.1029/2012EO440006, 2012
620

Bi, S., and Hieronymi, M.: Holistic optical water type classification for ocean, coastal, and inland waters, Limnol. Oceanogr., doi: 10.1002/lno.12606, 2024.

Bramich, J. M., Bolch, C. J., and Fischer, A. M.: Evaluation of atmospheric correction and high-resolution processing on
625   SeaDAS-derived chlorophyll-a: An example from mid-latitude mesotrophic waters, Int. J. Remote Sens., doi: 10.1080/01431161.2017.1420930, 2018.

Brockmann, C., Doerffer, R., Peters, M., Kerstin, S., Embacher, S., and Ruescas, A.: Evolution of the C2RCC neural network for Sentinel 2 and 3 for the retrieval of ocean color products in normal and extreme optically complex waters, Living Planet Symposium, Vol. 740, pp. 54, August, 2016.

Coddington, O. M., Richard, E. C., Harber, D., Pilewskie, P., Woods, T. N., Chance, K., Liu, X., and Sun, K.: The TSIS-1 hybrid solar reference spectrum, Geophys. Res. Lett., 48, e2020GL091709, doi:10.1029/2020GL091709, 2021.

Committee on Earth Observation Satellites: Product Family Specification, Aquatic Reflectance, version 1.0, CEOS, available at https://ceos.org/ard/index.html#specs, accessed April 2025, 2022.

Crawford, C. J., Roy, D. P., Arab, S., Barnes, C., Vermote, E., Hulley, G., Gerace, A., Choate, M., Engebretson, C., Micijevic, E., and Schmidt, G.: The 50-year Landsat collection 2 archive, Sci. Remote Sens., 8, 100103, doi: 10.1016/j.srs.2023.100103, 2023.

Crawford, C.J., Page, B.P., Arab, S., Schmidt, G., Barnes, C., Wellington, D.: In situ Radiometric Validation Data Record for Landsat 8/9 Operational Land Imager (OLI) Level 2 Aquatic Reflectance Products Version 1.0, ScienceBase, doi: 10.5066/P14RSMQD, 2025[1]

Crawford, C.J., Page, B.P., Arab, S., Schmidt, G., Barnes, C., Wellington, D.: Landsat 8-9 Operational Land Imager (OLI) Level 2 Provisional Aquatic Reflectance Products, Collection 2 Validation Subset, ScienceBase, doi: 10.5066/P14MBBRM, 2025[2]

Concha, J. A., and Schott, J. R.: Retrieval of color producing agents in Case 2 waters using Landsat 8, Remote Sens. Environ., 185, 95–107, doi: 10.1016/j.rse.2016.03.018, 2016.

Concha, J. A., Bracaglia, M., and Brando, V.E.: Assessing the influence of different validation protocols on Ocean Colour match-up analyses, Remote Sensing of Environment, 259, 112415, 2021, doi: 10.1016/j.rse.2021.112415.

Dash, P., Walker, N., Mishra, D., D'Sa, E., and Ladner, S.: Atmospheric correction and vicarious calibration of Oceansat-1 Ocean Color Monitor (OCM) data in coastal case 2 waters, Remote Sens., 4, 1716–1740, doi: 10.3390/rs4061716, 2012.

De Keukelaere, L., Sterckx, S., Adriaensen, S., Knaeps, E., Reusen, I., Giardino, C., Bresciani, M., Hunter, P., Neil, C., Van der Zande, D., and Vaiciute, D.: Atmospheric correction of Landsat-8/OLI and Sentinel-2/MSI data using iCOR algorithm: validation for coastal and inland waters, Eur. J. Remote Sens., 51, 525–542, doi: 10.1080/22797254.2018.1457937, 2018.

Dierssen, H. M., Zimmerman, R. C., Drake, L. A., and Burdige, D.: Benthic ecology from space: optics and net primary production in seagrass and benthic algae across the Great Bahama Bank, Mar. Ecol. Prog. Ser., 411, 1–15, doi: 10.3354/meps08665, 2010.

665

Dierssen, H. M., Ackleson, S. G., Joyce, K. E., Hestir, E. L., Castagna, A., Lavender, S., and McManus, M. A.: Living up to the hype of hyperspectral aquatic remote sensing: science, resources and outlook, Front. Environ. Sci., 9, 649528, doi: 10.3389/fenvs.2021.649528, 2021.

670   Dogliotti, A. I., Ruddick, K. G., Nechad, B., Doxaran, D., and Knaeps, E.: A single algorithm to retrieve turbidity from remotely-sensed data in all coastal and estuarine waters, Remote Sens. Environ., 156, 157–168, doi: 10.1016/j.rse.2014.09.020, 2015.

Dwyer, J. L., Roy, D. P., Sauer, B., Jenkerson, C. B., Zhang, H. K., and Lymburner, L.: Analysis ready data: enabling analysis
675   of the Landsat archive, Remote Sens., 10, 1363, doi: 10.3390/rs10091363, 2018.

Fan, Y., Li, W., Chen, N., Ahn, J. H., Park, Y. J., Kratzer, S., Schroeder, T., Ishizaka, J., Chang, R., and Stamnes, K.: OC-SMART: A machine learning based data analysis platform for satellite ocean color sensors, Remote Sens. Environ., 253, 112236, doi: 10.1016/j.rse.2020.112236, 2021.

680

Fickas, K. C., O'Shea, R. E., Pahlevan, N., Smith, B., Bartlett, S. L., and Wolny, J. L.: Leveraging multimission satellite data for spatiotemporally coherent cyanoHAB monitoring, Front. Remote Sens., 4, 1157609, doi: 10.3389/frsen.2023.1157609, 2023.

685   Franz, B. A., Bailey, S. W., Werdell, P. J., and McClain, C. R.: Sensor-independent approach to the vicarious calibration of satellite ocean color radiometry, Appl. Opt., 46, 5068–5082, doi: 10.1364/AO.46.005068, 2007.

Franz, B. A., Bailey, S. W., Kuring, N., and Werdell, P. J.: Ocean color measurements with the Operational Land Imager on Landsat-8: implementation and evaluation in SeaDAS, J. Appl. Remote Sens., 9, 096070, doi: 10.1117/1.JRS.9.096070, 2015.

690

GCOS: The 2022 GCOS ECVs Requirements, https://library.wmo.int/idurl/4/58111, 2022. Updated in 2025.

Giardino, C., Kõks, K. L., Bolpagni, R., Luciani, G., Candiani, G., Lehmann, M. K., Van der Woerd, H. J., and Bresciani, M.: The color of water from space: a case study for Italian lakes from Sentinel-2, Geospatial Anal. Earth Obs. Data, doi:
695   10.5772/intechopen.86596, 2019.

Gordon, H. R., and Wang, M.: Retrieval of water-leaving radiance and aerosol optical thickness over the oceans with SeaWiFS: a preliminary algorithm, Appl. Opt., 33, 443–452, doi: 10.1364/AO.33.000443, 1994.

700 He, X., Bai, Y., Pan, D., Tang, J., and Wang, D.: Atmospheric correction of satellite ocean color imagery using the ultraviolet wavelength for highly turbid waters, Opt. Express, 20, 20754–20770, doi: 10.1364/OE.20.020754, 2012.

He, Q., and Chen, C.: A new approach for atmospheric correction of MODIS imagery in turbid coastal waters: a case study for the Pearl River Estuary, Remote Sens. Lett., 5, 249–257, doi: 10.1080/2150704X.2014.898192, 2014.

705

Ibrahim, A., Franz, B. A., Ahmad, Z., and Bailey, S. W.: Multiband atmospheric correction algorithm for ocean color retrievals, Front. Earth Sci., 7, 116, doi: 10.3389/feart.2019.00116, 2019.

Ilori, C. O., Pahlevan, N., and Knudby, A.: Analyzing performances of different atmospheric correction techniques for Landsat 710 8: Application for coastal remote sensing, Remote Sens., 11, 469, doi: 10.3390/rs11040469, 2019.

IOCCG Technical Series, Jamet, C. (ed.): Atmospheric Correction over turbid waters, IOCCG, Vol. 1.0, Dartmouth, NS, Canada, 2019.

715 Johnson, B.C. and Zibordi, G. et al.: Characterization and absolute calibration of an AERONET-OC radiometer, Appl. Opt., 60, 3380–3392, doi: 10.1364/AO.419766, 2021.

Joshi, I. D. and D'Sa, E. J.: Optical properties using adaptive selection of NIR/SWIR reflectance correction and quasi-analytic algorithms for the MODIS-Aqua in estuarine-ocean continuum: application to the northern Gulf of Mexico, IEEE Trans. 720 Geosci. Remote Sens., 58, 6088–6105, doi:10.1109/TGRS.2020.2973157, 2020.

Korkin, S., and Lyapustin, A.: Radiative interaction of atmosphere and surface: Write-up with elements of code, J. Quant. Spectrosc. Radiat. Transfer, 309, 108663, doi: 10.1016/j.jqsrt.2023.108663, 2023.

725 Kuhn, C., de Matos Valerio, A., Ward, N., Loken, L., Sawakuchi, H. O., Kampel, M., Richey, J., Stadler, P., Crawford, J., Striegl, R., and Vermote, E.: Performance of Landsat-8 and Sentinel-2 surface reflectance products for river remote sensing retrievals of chlorophyll-a and turbidity, Remote Sens. Environ., 224, 104–118, doi: 10.1016/j.rse.2019.01.023, 2019.

Lee, Z., Carder, K. L., Steward, R. G., Peacock, T. G., Davis, C. O., and Mueller, J. L.: Remote sensing reflectance and inherent optical properties of oceanic waters derived from above-water measurements, Ocean Opt. XIII, Vol. 2963, 160–166, doi: 10.1117/12.266436, February, 1997.

Lee, Z., Carder, K. L., Chen, R. F., and Peacock, T. G.: Properties of the water column and bottom derived from Airborne Visible Infrared Imaging Spectrometer (AVIRIS) data, J. Geophys. Res., 106, 11639–11651, doi: 10.1029/2000JC000554, 2001.

Lehmann, M. K., Nguyen, U., Allan, M., and Van der Woerd, H. J.: Colour classification of 1486 lakes across a wide range of optical water types, Remote Sens., 10, 1273, doi: 10.3390/rs10081273, 2018.

Lehmann, M. K., Gurlin, D., Pahlevan, N., Alikas, K., Conroy, T., Anstee, J., Balasubramanian, S. V., Barbosa, C. C., Binding, C., Bracher, A., and Bresciani, M.: GLORIA-A globally representative hyperspectral in situ dataset for optical sensing of water quality, Sci. Data, 10, 100, doi(1): 10.1038/s41597-023-02069-3, doi(2); 10.1594/PANGAEA.948492, 2023.

Lekki, J., Deutsch, E., Sayers, M., Bosse, K., Anderson, R., Tokars, R., and Sawtell, R.: Determining remote sensing spatial resolution requirements for the monitoring of harmful algal blooms in the Great Lakes, J. Great Lakes Res., 45, 434–443, doi: 10.1016/j.jglr.2019.03.014, 2019.

Liu, H., Zhou, Q., Li, Q., Hu, S., Shi, T., and Wu, G.: Determining switching threshold for NIR-SWIR combined atmospheric correction algorithm of ocean color remote sensing, ISPRS J. Photogramm. Remote Sens., 153, 59–73, doi:10.1016/j.isprsjprs.2019.04.013, 2019.

Louchard, E. M., Reid, R. P., Stephens, F. C., Davis, C. O., Leathers, R. A., and Valerie, T. D.: Optical remote sensing of benthic habitats and bathymetry in coastal environments at Lee Stocking Island, Bahamas: A comparative spectral classification approach, Limnol. Oceanogr., 48, 511–521, doi: 10.4319/lo.2003.48.1_part_2.0511, 2003.

Mannino, A.: Landsat 8's Atmospheric Correction in SeaDAS: Comparison with AERONET-OC, J. Sci. Res., 2016.

Mao, Z., Chen, J., Hao, Z., Pan, D., Tao, B., and Zhu, Q.: A new approach to estimate the aerosol scattering ratios for the atmospheric correction of satellite remote sensing data in coastal regions, Remote Sens. Environ., 132, 186–194, doi: 10.1016/j.rse.2013.01.015, 2013.

Mélin, F., Zibordi, G., Berthon, J. F., Bailey, S., Franz, B., Voss, K., Flora, S., and Grant, M.: Assessment of MERIS reflectance data as processed with SeaDAS over the European seas, Opt. Express, 19, 25657–25671, doi: 10.1364/OE.19.025657, 2011.

Meyer, M. F., Topp, S. N., King, T. V., Ladwig, R., Pilla, R. M., Dugan, H. A., Eggleston, J. R., Hampton, S. E., Leech, D. M., Oleksy, I. A., and Ross, J. C.: National-scale remotely sensed lake trophic state from 1984 through 2020, Sci. Data, 11, 77, doi: 10.6073/pasta/212a3172ac36e8dc6e1862f9c2522fa4, 2024.

Mishra, S., and Mishra, D. R.: Normalized difference chlorophyll index: A novel model for remote estimation of chlorophyll-a concentration in turbid productive waters, Remote Sens. Environ., 117, 394–406, doi: 10.1016/j.rse.2011.10.016, 2012.

Mobley, C. D.: Estimation of the remote-sensing reflectance from above-surface measurements, Appl. Opt., 38, 7442–7455, doi: 10.1364/AO.38.007442, 1999.

Mobley, C. D., Werdell, J., Franz, B., Ahmad, Z., and Bailey, S.: Atmospheric correction for satellite ocean color radiometry, NASA GSFC-E-DAA-TN35509, 2016.

Moore, T. S., Feng, H., Ruberg, S. A., Beadle, K., Constant, S. A., Miller, R., Muzzi, R. W., Johengen, T. H., DiGiacomo, P. M., Lance, V. P., and Holben, B. N.: SeaPRISM observations in the western basin of Lake Erie in the summer of 2016, J. Great Lakes Res., 45, 547–555, doi: 10.1016/j.jglr.2018.10.008, 2019.

Moses, W. J., Sterckx, S., Montes, M. J., De Keukelaere, L., and Knaeps, E.: Atmospheric correction for inland waters, Bio-optical Model. Remote Sens. Inland Waters, Elsevier, pp. 69–100, doi: 10.1016/B978-0-12-804644-9.00003-3, 2017.

Nazeer, M., Bilal, M., Nichol, J. E., Wu, W., Alsahli, M. M., Shahzad, M. I., and Gayen, B. K.: First experiences with the Landsat-8 aquatic reflectance product: evaluation of the regional and ocean color algorithms in a coastal environment, Remote Sens., 12, 1938, doi: 10.3390/rs12121938, 2020.

Niroumand-Jadidi, M., Bovolo, F., Bresciani, M., Gege, P., and Giardino, C.: Water quality retrieval from Landsat-9 (OLI-2) imagery and comparison to Sentinel-2, Remote Sens., 14, 4596, doi: 10.3390/rs14184596, 2022.

Ogashawara, I., Jechow, A., Kiel, C., Kohnert, K., Berger, S. A., and Wollrab, S.: Performance of the Landsat 8 provisional aquatic reflectance product for inland waters, Remote Sens., 12, 2410, doi: 10.3390/rs12152410, 2020.

Ogashawara, I., Wollrab, S., Berger, S. A., Kiel, C., Jechow, A., Guislain, A. L., Gege, P., Ruhtz, T., Hieronymi, M., Schneider, T., and Lischeid, G.: Unleashing the power of remote sensing data in aquatic research: Guidelines for optimal utilization, Limnol. Oceanogr. Lett., 9, 667–673, doi: 10.1002/lol2.10427, 2024.

Olmanson, L. G., Brezonik, P. L., Finlay, J. C., and Bauer, M. E.: Comparison of Landsat 8 and Landsat 7 for regional measurements of CDOM and water clarity in lakes, Remote Sens. Environ., 185, 119–128, doi: 10.1016/j.rse.2016.01.007, 2016.

O'Reilly, J. E., Maritorena, S., Mitchell, B. G., Siegel, D. A., Carder, K. L., Garver, S. A., Kahru, M., and McClain, C.: Ocean color chlorophyll algorithms for SeaWiFS, J. Geophys. Res. Oceans, 103, 24937–24953, doi: 10.1029/98JC02160, 1998.

Pahlevan, N., and Schott, J. R.: Characterizing the relative calibration of Landsat-7 (ETM+) visible bands with Terra (MODIS) over clear waters: The implications for monitoring water resources, Remote Sens. Environ., 125, 167–180, doi:10.1016/j.rse.2012.07.013, 2012.

Pahlevan, N., Lee, Z., Wei, J., Schaaf, C. B., Schott, J. R., and Berk, A.: On-orbit radiometric characterization of OLI (Landsat-8) for applications in aquatic remote sensing, Remote Sens. Environ., 154, 272–284, doi: 10.1016/j.rse.2014.08.001, 2014.

Pahlevan, N., Schott, J. R., Franz, B. A., Zibordi, G., Markham, B., Bailey, S., Schaaf, C. B., Ondrusek, M., Greb, S., and Strait, C. M.: Landsat 8 remote sensing reflectance (Rrs) products: Evaluations, intercomparisons, and enhancements, Remote Sens. Environ., 190, 289–301, doi: 10.1016/j.rse.2016.12.030, 2017.

Pahlevan, N., Balasubramanian, S. V., Sarkar, S., and Franz, B. A.: Toward long-term aquatic science products from heritage Landsat missions, Remote Sens., 10, 1337, doi: 10.3390/rs10091337, 2018.

Pahlevan, N., Chittimalli, S. K., Balasubramanian, S. V., and Vellucci, V.: Sentinel-2/Landsat-8 product consistency and implications for monitoring aquatic systems, Remote Sens. Environ., 220, 19–29, doi: 10.1016/j.rse.2018.10.027, 2019.

Pahlevan, N., Mangin, A., Balasubramanian, S. V., Smith, B., Alikas, K., Arai, K., Barbosa, C., Bélanger, S., Binding, C., Bresciani, M., and Giardino, C.: ACIX-Aqua: A global assessment of atmospheric correction methods for Landsat-8 and Sentinel-2 over lakes, rivers, and coastal waters, Remote Sens. Environ., 258, 112366, doi: 10.1016/j.rse.2021.112366, 2021.

Pahlevan, N., Smith, B., Alikas, K., Anstee, J., Barbosa, C., Binding, C., Bresciani, M., Cremella, B., Giardino, C., Gurlin, D., and Fernandez, V.: Simultaneous retrieval of selected optical water quality indicators from Landsat-8, Sentinel-2, and Sentinel-3, Remote Sens. Environ., 270, 112860, doi: 10.1016/j.rse.2021.112860, 2022.

830   Pinnel, N., Langheinrich, M., Soppa, M. A., Randrianalisoa, A. N., Alvarado, L., Gege, P., de los Reyes, R., Heege, T., Bracher, A., Pato, M., and Habermeyer, M.: Hyperspectral EnMAP Data Processing for aquatic science and applications, J. Sci. Res., 2024.

Pellegrino, A., Fabbretto, A., Bresciani, M., de Lima, T.M.A., Braga, F., Pahlevan, N., Brando, V.E., Kratzer, S., Gianinetto,
835   M. and Giardino, C.: Assessing the accuracy of PRISMA standard reflectance products in globally distributed aquatic sites, Remote Sensing, 15, 2163, doi: [insert DOI if available], 2023.

Poppenga, S. K., and Danielson, J. J.: A comparison of Landsat 8 Operational Land Imager and Provisional Aquatic Reflectance science product, Sentinel–2B, and WorldView–3 imagery for empirical satellite-derived bathymetry, Unalakleet,
840   Alaska, US Geological Survey, No. 2021–5097, doi: 10.3133/sir20215097, 2021.

Radeloff, V. C., Roy, D. P., Wulder, M. A., Anderson, M., Cook, B., Crawford, C. J., Friedl, M., Gao, F., Gorelick, N., Hansen, M., and Healey, S.: Need and vision for global medium-resolution Landsat and Sentinel-2 data products, Remote Sens. Environ., 300, 113918, doi: 10.1016/j.rse.2023.113918, 2024.
845

Roy, D. P., Wulder, M. A., Loveland, T. R., Woodcock, C. E., Allen, R. G., Anderson, M. C., Helder, D., Irons, J. R., Johnson, D. M., Kennedy, R., and Scambos, T. A.: Landsat-8: Science and product vision for terrestrial global change research, Remote Sens. Environ., 145, 154–172, doi: 10.1016/j.rse.2014.02.001, 2014.

850   Ruddick, K. G., Ovidio, F., and Rijkeboer, M.: Atmospheric correction of SeaWiFS imagery for turbid coastal and inland waters, Appl. Opt., 39, 897–912, doi: 10.1364/AO.39.000897, 2000.

Seegers, B. N., Stumpf, R. P., Schaeffer, B. A., Loftin, K. A., and Werdell, P. J.: Performance metrics for the assessment of satellite data products: an ocean color case study, Opt. Express, 26, 7404–7422, doi: 10.1364/OE.26.007404, 2018.
855

Schott, J. R., Gerace, A., Woodcock, C. E., Wang, S., Zhu, Z., Wynne, R. H., and Blinn, C. E.: The impact of improved signal-to-noise ratios on algorithm performance: Case studies for Landsat class instruments, Remote Sens. Environ., 185, 37–45, doi:10.1016/j.rse.2016.04.015, 2016.

860   Singh, R.K., and Shanmugam, P.: A novel method for estimation of aerosol radiance and its extrapolation in the atmospheric correction of satellite data over optically complex oceanic waters, Remote Sensing of Environment, 142, 188–206, doi:10.1016/j.rse.2013.12.008, 2014.

Steinmetz, F., Deschamps, P. Y., and Ramon, D.: Atmospheric correction in presence of sun glint: application to MERIS, Opt.
865 Express, 19, 9783–9800, doi: 10.1364/OE.19.009783, 2011.

Steinmetz, F., and Ramon, D.: Sentinel-2 MSI and Sentinel-3 OLCI consistent ocean colour products using POLYMER, Remote Sens. Open Coastal Ocean Inland Waters, Vol. 10778, 46–55, doi: 10.1117/12.2500232, October, 2018.

870 Stengel, V. G., Trevino, J. M., King, T. V., Ducar, S. D., Hundt, S. A., Hafen, K. C., and Churchill, C. J.: Near real-time satellite detection and monitoring of aquatic algae and cyanobacteria: how a combination of chlorophyll-a indices and water-quality sampling was applied to north Texas reservoirs, J. Appl. Remote Sens., 17, 044514, doi: 10.1117/1.JRS.17.044514, 2023.

875 Spyrakos, E., O'Donnell, R., Hunter, P. D., Miller, C., Scott, M., Simis, S. G., Neil, C., Barbosa, C. C., Binding, C. E., Bradt, S., and Bresciani, M.: Optical types of inland and coastal waters, Limnol. Oceanogr., 63, 846–870, doi: 10.1002/lno.10674, 2018.

Tavora, J., Jiang, B., Kiffney, T., Bourdin, G., Gray, P.C., de Carvalho, L.S., Hesketh, G., Schild, K.M., Faria de Sousa, L.,
880 Brady, D.C. and Boss, E.: Recipes for the derivation of water quality parameters using the high-spatial-resolution data from sensors on board Sentinel-2A, Sentinel-2B, Landsat-5, Landsat-7, Landsat-8, and Landsat-9 satellites, J. Remote Sens., 3, 49, doi: 10.34133/remotesensing.0049, 2023.

Thompson, D. R., Cawse-Nicholson, K., Erickson, Z., Fichot, C. G., Frankenberg, C., Gao, B. C., and Thompson, A.: A unified
885 approach to estimate land and water reflectances with uncertainties for coastal imaging spectroscopy, Remote Sens. Environ., 231, 111198, doi:10.1016/j.rse.2019.05.017, 2019.

Thompson, D.R., Guanter, L., Berk, A., Gao, B.C., Richter, R., Schläpfer, D. and Thome, K.J.: Retrieval of atmospheric parameters and surface reflectance from visible and shortwave infrared imaging spectroscopy data, Surv. Geophys., 40, 333–
890 360, doi: 10.1007/s10712-018-9488-9, 2019.

Thompson, D.R., Bohn, N., Brodrick, P.G., Carmon, N., Eastwood, M.L., Eckert, R., Fichot, C.G., Harringmeyer, J.P., Nguyen, H.M., Simard, M. and Thorpe, A.K.: Atmospheric lengthscales for global VSWIR imaging spectroscopy, J. Geophys. Res. Biogeosci., 127, e2021JG006711, doi: 10.1029/2021JG006711, 2022.
895

Thuillier, G., Hersé, M., Labs, D., Foujols, T., Peetermans, W., Gillotay, D., Simon, P.C. and Mandel, H.: The solar spectral irradiance from 200 to 2400 nm as measured by the SOLSPEC spectrometer from the ATLAS and EURECA missions, Sol. Phys., 214, 1–22, doi: 10.1023/A:1024048429145, 2003.

900 Tyler, A., Hunter, P., De Keukelaere, L., Ogashawara, I. and Spyrakos, E.: Remote Sensing of Inland Water Quality, 2022.

Vanhellemont, Q., Bailey, S., Franz, B. and Shea, D.: Atmospheric correction of Landsat-8 imagery using SeaDAS, ESA Spec. Publ., 726, 2014.

USGS: Landsat 8-9 Collection 2 Level-2 Provisional Aquatic Reflectance Algorithm Description Document,
905 https://www.usgs.gov/media/files/landsat-8-9-collection-2-level-2-provisional-aquatic-reflectance-algorithm-description, 2024.

USGS: Landsat Next Fact Sheet 2024-3005, https://pubs.usgs.gov/fs/2024/3005/fs20243005.pdf, doi: 10.3133/fs2024005. 2024

910

USGS: Landsat 8-9 Collection 2 Level-2 Provisional Aquatic Reflectance Product Guide, https://www.usgs.gov/media/files/landsat-8-9-collection-2-level-2-provisional-aquatic-reflectance-product-guide, 2025.

Vanhellemont, Q., and Ruddick, K.: Advantages of high-quality SWIR bands for ocean colour processing: Examples from
915 Landsat-8, Remote Sens. Environ., 161, 89–106, doi:10.1016/j.rse.2015.02.007, 2015.

Vanhellemont, Q., and Ruddick, K.: Atmospheric correction of metre-scale optical satellite data for inland and coastal water applications, Remote Sens. Environ., 216, 586–597, doi:10.1016/j.rse.2018.07.015, 2018.

920 Vanhellemont, Q.: Adaptation of the dark spectrum fitting atmospheric correction for aquatic applications of the Landsat and Sentinel-2 archives, Remote Sens. Environ., 225, 175–192, doi: 10.1016/j.rse.2019.03.010, 2019.

Vermote, E.F. and Kotchenova, S.: Atmospheric correction for the monitoring of land surfaces, J. Geophys. Res. Atmos., 113, D23, doi: 10.1029/2007JD009662, 2008.
925

Wang, M. and Shi, W.: The NIR-SWIR combined atmospheric correction approach for MODIS ocean color data processing, Opt. Express, 15, 15722–15733, doi: 10.1364/OE.15.015722, 2007.

Wang, M.: Atmospheric correction for remotely-sensed ocean-colour products, Reports and Monographs of the International
Ocean-Colour Coordinating Group (IOCCG), 2010.

Wang, M., and Gordon, H. R.: Sensor performance requirements for atmospheric correction of satellite ocean color remote sensing, Opt. Express, 26(6), 7390–7403, doi:10.1364/OE.26.007390, 2018.

Wang, J., Wang, Y., Lee, Z., Wang, D., Chen, S. and Lai, W.: A revision of NASA SeaDAS atmospheric correction algorithm over turbid waters with artificial Neural Networks estimated remote-sensing reflectance in the near-infrared, ISPRS J. Photogramm. Remote Sens., 194, 235–249, doi: 10.1016/j.isprsjprs.2022.10.014, 2022.

Wei, J., Lee, Z., Garcia, R., Zoffoli, L., Armstrong, R.A., Shang, Z., Sheldon, P. and Chen, R.F.: An assessment of Landsat-8 atmospheric correction schemes and remote sensing reflectance products in coral reefs and coastal turbid waters, Remote Sens. Environ., 215, 18–32, doi: 10.1016/j.rse.2018.05.033, 2018.

Wei, J., Wang, M., Ondrusek, M., Gilerson, A., Goes, J., Hu, C., Lee, Z., Voss, K.J., Ladner, S., Lance, V.P. and Tufillaro, N.: Satellite ocean color validation, Field Meas. Passive Environ. Remote Sens., Elsevier, 351–374, doi: 10.1016/B978-0-12-823953-7.00006-X, 2023.

Wei, J., Wang, M., Jiang, L., Lee, Z., Kirby, R., Mikelsons, K., and Lin, G.: Satellite observations of water transparency from VIIRS in global aquatic ecosystems, Remote Sensing of Environment, 330, 114981, doi: 10.1016/j.rse.2025.114981.

Werdell, P. J., and Bailey, S. W.: An improved in-situ bio-optical data set for ocean color algorithm development and satellite data product validation, Remote Sens. Environ., 98(1), 122–140, doi:10.1016/j.rse.2005.07.001, 2005.

Werdell, P.J., Franz, B.A., Bailey, S.W., Harding Jr, L.W. and Feldman, G.C.: Approach for the long-term spatial and temporal evaluation of ocean color satellite data products in a coastal environment, Coastal Ocean Remote Sens., SPIE, 6680, 115–126, doi: 10.1117/12.732489, 2007.

Werdell, P.J., Franz, B.A. and Bailey, S.W.: Evaluation of shortwave infrared atmospheric correction for ocean color remote sensing of Chesapeake Bay, Remote Sens. Environ., 114, 2238–2247, doi: 10.1016/j.rse.2010.04.027, 2010.

Wu, Y., Knudby, A., Pahlevan, N., Lapen, D., and Zeng, C.: Sensor-generic adjacency-effect correction for remote sensing of coastal and inland waters, Remote Sens. Environ., 315, 114433, doi:10.1016/j.rse.2024.114433, 2024.

Wulder, M.A., Loveland, T.R., Roy, D.P., Crawford, C.J., Masek, J.G., Woodcock, C.E., Allen, R.G., Anderson, M.C., Belward, A.S., Cohen, W.B. and Dwyer, J.: Current status of Landsat program, science, and applications, Remote Sens. Environ., 225, 127–147, doi: 10.1016/j.rse.2010.04.027, 2019.

Wulder, M.A., Roy, D.P., Radeloff, V.C., Loveland, T.R., Anderson, M.C., Johnson, D.M., Healey, S., Zhu, Z., Scambos, T.A., Pahlevan, N. and Hansen, M.: Fifty years of Landsat science and impacts, Remote Sens. Environ., 280, 113195, doi:XXXXXX, 2022.

Xu, Y., Feng, L., Zhao, D. and Lu, J.: Assessment of Landsat atmospheric correction methods for water color applications using global AERONET-OC data, Int. J. Appl. Earth Obs. Geoinf., 93, 102192, doi: 10.1016/j.rse.2022.113195, 2020.

Yan, N., Sun, Z., Huang, W., Jun, Z. and Sun, S.: Assessing Landsat-8 atmospheric correction schemes in low to moderate turbidity waters from a global perspective, Int. J. Digit. Earth, 16, 66–92, doi: 10.1080/17538947.2022.2161651, 2023.

Zhu, Z., Wang, S. and Woodcock, C.E.: Improvement and expansion of the Fmask algorithm: Cloud, cloud shadow, and snow detection for Landsats 4–7, 8, and Sentinel-2 images, Remote Sens. Environ., 159, 269–277, doi: 10.1016/j.rse.2014.12.014, 2015.

Zhu, Z., Wulder, M.A., Roy, D.P., Woodcock, C.E., Hansen, M.C., Radeloff, V.C., Healey, S.P., Schaaf, C., Hostert, P., Strobl, P. and Pekel, J.F.: Benefits of the free and open Landsat data policy, Remote Sens. Environ., 224, 382–385, doi: 10.1016/j.rse.2019.02.016, 2019.

Zibordi, G., Holben, B., Hooker, S.B., Mélin, F., Berthon, J.F., Slutsker, I., Giles, D., Vandemark, D., Feng, H., Rutledge, K. and Schuster, G.: A network for standardized ocean color validation measurements, Eos Trans. Am. Geophys. Union, 87, 293–297, doi: 10.1029/2006EO300001, 2006.

Zibordi, G., Mélin, F., Berthon, J.F., Holben, B., Slutsker, I., Giles, D., D'Alimonte, D., Vandemark, D., Feng, H., Schuster, G. and Fabbri, B.E.: AERONET-OC: a network for the validation of ocean color primary products, J. Atmos. Oceanic Technol., 26, 1634–1651, doi: 10.1175/2009JTECHO654.1, 2009.